THE JOURNAL OF BIOLOGICAL CHEMISTRY VOL. 291, NO. 9, pp. 4763–4778, February 26, 2016

Adverse Outcomes Associated with Cigarette Smoke Radicals Related to Damage to Protein-disulfide Isomerase*

Received for publication, December 22, 2015, and in revised form, January 3, 2016 Published, JBC Papers in Press, January 4, 2016, DOI 10.1074/jbc.M115.712331

Harshavardhan Kenche[‡1], Zhi-Wei Ye[§1], Kokilavani Vedagiri[‡], Dylan M. Richards[‡], Xing-Huang Gao[¶], Kenneth D. Tew[§], Danyelle M. Townsend[§], and Anna Blumental-Perry[‡‖2]**

*From the [‡]Anderson Cancer Institute, Memorial Health University Medical Center, Savannah, Georgia 31404, the [‖]Department of Biomedical Sciences, Mercer University School of Medicine, Savannah, Georgia 31404, the Departments of **Surgery and [¶]Genetics, Case Western Reserve University, Cleveland, Ohio 44106, and the [§]College of Pharmacy, Medical University of South Carolina, Charleston, South Carolina 29425*

Identification of factors contributing to the development of chronic obstructive pulmonary disease (COPD) is crucial for developing new treatments. An increase in the levels of protein-disulfide isomerase (PDI), a multifaceted endoplasmic reticulum resident chaperone, has been demonstrated in human smokers, presumably as a protective adaptation to cigarette smoke (CS) exposure. We found a similar increase in the levels of PDI in the murine model of COPD. We also found abnormally high levels (4–6 times) of oxidized and sulfenilated forms of PDI in the lungs of murine smokers compared with non-smokers. PDI oxidation progressively increases with age. We begin to delineate the possible role of an increased ratio of oxidized PDI in the age-related onset of COPD by investigating the impact of exposure to CS radicals, such as acrolein (AC), hydroxyquinones (HQ), peroxynitrites (PN), and hydrogen peroxide, on their ability to induce unfolded protein response (UPR) and their effects on the structure and function of PDIs. Exposure to AC, HQ, PN, and CS resulted in cysteine and tyrosine nitrosylation leading to an altered three-dimensional structure of the PDI due to a decrease in helical content and formation of a more random coil structure, resulting in protein unfolding, inhibition of PDI reductase and isomerase activity *in vitro* and *in vivo*, and subsequent induction of endoplasmic reticulum stress response. Addition of glutathione prevented the induction of UPR, and AC and HQ induced structural changes in PDI. Exposure to PN and glutathione resulted in conjugation of PDI possibly at active site tyrosine residues. The findings presented here propose a new role of PDI in the pathogenesis of COPD and its age-dependent onset.

Few threats to public health are as onerous as tobacco; nevertheless, smoking is still a widespread phenomenon. More than 435,000 Americans die each year of tobacco-related pulmonary illnesses. Chronic obstructive pulmonary disease (COPD)[3] is one such illness, ranked the third leading cause of tobacco-related morbidity and mortality worldwide in 2012, claiming the lives of over 3 million people, with an economic cost of 2.1 trillion dollars (1–3). Moreover, the number of COPD deaths will increase significantly reaching a predicted 4.5 million in 2020 (4). This strongly supports the need for an in-depth study on COPD, because currently, there are no effective treatments that can cure COPD or stop its progression. Exposure to cigarette smoke (CS) is a major risk factor for the development of COPD (5, 6). Upon inhalation of CS, the free radicals in it reach the interior of lung cells, where they can react with a wide variety of proteins and prevent them from functioning properly. We and others previously demonstrated that exposure to CS interferes with the function of the endoplasmic reticulum (ER) and elicits the unfolded protein response (UPR) (7–14). UPR is a proteostasis-regulating system that originates from the ER. UPR is initiated upon activation of one or a combination of either three major ER-transmembrane proteins that sense the homeostatic state of the ER as follows: 1) protein kinase RNA-like endoplasmic reticulum kinase (PERK); 2) activating transcription factor 6 (ATF6); and 3) kinase and ribonuclease inositol-requiring enzyme 1 (IRE1) (15–17). We demonstrated that initial UPR induction in the lungs of smokers occurs via the PERK pathway as manifested by phosphorylation of eIF2α and via activation of ATF6 (18).

We previously identified protein-disulfide isomerase (PDI) as a primary ER-resident target of CS-induced oxidation; its malfunction may be a potential cause of CS-induced UPR. PDI is one of the abundant ER luminal proteins with multiple functions (19, 20). It is a molecular chaperone and a major component in disulfide bond formation and isomerization systems (21). Disulfide bonds are extremely important for overall three-dimensional structure and therefore for the functioning of most secreted proteins, which compose ~30% of all proteins. As

* This work was supported by Flight Attendants Medical Research Institute Young Clinical Investigator Award 092207 (to A. B. P.), National Institutes of Health Grants 5P20GM103542 from NCRR, from COBRE in Oxidants, Redox Balance and Stress Signaling (to D. M. T.), C06 RR015455 (to K. D. T.), and R37-DK60596 and R01-DK53307 (to Maria Hatzoglou). The authors declare that they have no conflicts of interest with the contents of this article. The content is solely the responsibility of the authors and does not necessarily represent the official views of the National Institutes of Health.

[1] Both authors contributed equally to this work.

[2] To whom correspondence should be addressed: Dept. of Surgery, Case Western Reserve University, 2109 Adelbert Rd., Biomedical Research Bldg., Room 821, Cleveland, OH 44106. Tel.: 216-368-3150; Fax: 216-368-4223; E-mail: axb811@case.edu.

[3] The abbreviations used are: COPD, chronic obstructive pulmonary disease; PDI, protein-disulfide isomerase; ER, endoplasmic reticulum; CS, cigarette smoke; AC, acrolein; HQ, hydroxyquinone; PN, peroxynitrite; UPR, unfolded protein response; CSE, CS extract; NAC, *N*-acetyl-L-cysteine; HMWC, high molecular weight protein complex; DCP, 3-(2,4-dioxocyclohexyl)propyl 5-((3*aR*,6*S*,6*aS*)-hexahydro-2-oxo-1*H*-thieno[3,4-d]imidazol-6-yl)pentanoate; DrRNase, denatured and reduced RNase; PERK, protein kinase RNA-like endoplasmic reticulum kinase.

such, PDI function is essential for cell viability, and factors that affect it can lead to cell death due to multiple reasons. In addition to its roles and localization to the ER, minute fractions of PDI are detectable in cytosol, plasma membrane, and mitochondria. The functionality and the means by which PDI is transported to non-ER locations is less well understood, but it has been proposed that non-ER PDI might play a role in redox signaling or may associate with and regulate the activity of other proteins in these respective compartments (22). PDI is a highly evolutionarily conserved multidomain protein containing four thioredoxin-like domains called a, b, b′, and a′ and a C-terminal acidic region with a KDEL motif. Domains a and a′ each contain one active site Cys-Gly-His-Cys (23, 24). This active site conserves cysteines residues that mediate the disulfide bond formation through oxidation, isomerization, and reduction reactions between cysteines on client proteins. Domains of PDI are spatially organized in the shape of a twisted "U" with the a and a′ domains looking outward and participating in disulfide isomerization and the b domains forming the base and participating in substrate binding. Under physiological conditions, PDI activity is tightly regulated (25, 26). It has been shown that post-translational modifications on the active site cysteines and residues within their vicinity regulate PDI activity (19, 27). These post-translational modifications can be the result of physiological oxidation or as a consequence of several stresses. Physiological oxidation is usually reversible (27). For example, nitrosative stress due to endogenous NO during numerous disease states or due to drug administration can induce PDI *S*-nitrosylation in the form of reversible *S*-sulfenic and even irreversible *S*-sulfonic acid formation, as well as PDI *S*-glutathionylation (19, 28). Reversible *S*-glutathionylation has been shown in some systems to serve as a protector of reversible oxidized PDI from further irreversible oxidation (19). Low density lipoproteins or 4-hydroxynonenal cause PDI carbonylation (29). Most of these post-translational modifications blunt PDI enzymatic activity. Therefore, the induction of PDI post-translational modifications is a common way to control PDI activity during physiological stresses (20, 30). Severe and long lasting inhibition of PDI activity can lead to ER stress with the induction of UPR and the potentiation of apoptosis (20). These processes emerging in the pathogenesis of multiple diseases, such as neurodegenerative diseases, diabetes, etc. (28). In contrast, inhibition of PDI becomes a goal in the development of new anticancer drugs because tumors up-regulate PDI expression as a protective mechanism (31) and because an elevated amount of PDI usually confers protection from the stress in various diseases (32).

PDI is up-regulated in non-COPD smokers, presumably as a part of adaptation to CS exposure (10). CS is a mixture of over 4000 different compounds (33, 34). Which of those compounds are responsible for PDI oxidation and how this oxidation affects PDI three-dimensional structure and function are not known. Among those components are reactive oxygen species and reactive nitrogen species, such as hydrogen peroxide (H_2O_2), peroxynitrites (PN), and free radicals of organic compounds such as acrolein (AC) and hydroxyquinones (HQ) (35–37). All of these radicals potentially can cause PDI oxidation and lead to UPR induction. Although endogenous H_2O_2 is important for stimulating PDI enzymatic activity (38–40), nothing is known about exogenous H_2O_2, which is also a part of oxidative challenges to the cell. *S*-Nitrosylation of PDI has been implicated in some conditions such as Parkinson and Alzheimer diseases, but it is not clear whether CS-derived H_2O_2 and PN reach the ER and have effects on the function of PDI located in the ER (41).

Acrolein is a very reactive unsaturated aldehyde, highly electrophilic, and will react with cellular nucleophiles, particularly thiols. Quinones, which are aromatic organic compounds, are long lived and stable; they undergo immediate oxidation and in reactions that lead to the formation of superoxide radicals, hydrogen peroxide, and hydroxyl radicals, all of which can cause thiol modifications (34, 36). All of these radicals potentially can cause PDI oxidation and lead to UPR induction, but nothing is known about their effects on PDI. Therefore, we analyzed the dynamics of PDI expression in the murine model of COPD and the ability of CS radicals to cause oxidation of ER-resident PDI.

Materials and Methods

Reagents—Hydrogen peroxide was purchased from Fisher; peroxynitrites were from EMD Millipore. Acrolein, hydroquinone, *N*-acetyl-L-cysteine (NAC), and glutathione (reduced) were purchased from Sigma. The concentrations used in this study are 50 or 300 μM HQ, 30 or 60 μM AC, 40 or 100 μM PN, and 100 or 200 μM H_2O_2. Phosphatase inhibitor cocktails 2 and 3 and DMSO were from Sigma. Neutral Red assay kit was from Sigma. Protease inhibitor tablets were purchased from Roche Applied Science. Recombinant human PDI was purchased from Enzo Life Sciences. Antibodies were purchased from the following vendors: anti-PDI Clone 1-D-3 (Enzo Life Sciences); anti-PDI Clone RL-77 (Thermo Pierce); eIF2α-P (Cell Signaling Technologies); anti-glutathionylation (Virogen); and anti-nitrocysteine and anti-nitrotyrosine (US Biologicals). Secondary antibodies were from Pierce. DCP-Bio1 (3-(2,4-Dioxocyclohexyl)propyl 5-((3*aR*,6*S*,6*aS*)-hexahydro-2-oxo-1*H*-thieno[3,4-d]imidazol-6-yl)pentanoate) (DCP-Bio1) for sulfenic acid detection assays was purchased from KeraFAST, Inc.

Cell Culture—MLE12 cells were purchased from American Type Cell Culture (ATCC) and cultured in RPMI 1640 medium (CellGro) and supplemented with 4% fetal bovine serum (FBS) (Serum Source International), insulin/transferrin/selenous acid (ITS) premix (BD Biosciences), 10 nM hydrocortisone (Sigma), 10 nM β-estradiol (Sigma), 10 mM HEPES, 2 mM glutamine (CellGro), 100 units/ml penicillin, and 100 μg/ml streptomycin. All experiments were performed on cells between passages 2 and 12.

CS Extract (CSE) Preparation—CSE was prepared by modification of the protocol described by Carp and Janoff (42) and previously used by Kenche *et al.* (18). Briefly, 5 ml of RPMI 1640 medium (CellGro) was placed into a 15-ml conical tube, and the tube opening was sealed using parafilm. Two small openings were made in the paraffin cover; through one opening a 1-ml serological pipette (unfiltered) was inserted into the medium close to the bottom of the tube, and the other opening served as a vent. Tubings connected a three-way valve, with the end of a 1-ml serological pipette from one direction and a holder for unfiltered cigarette (Research Cigarettes, University of Ken-

tucky Tobacco Research Institute) connected to a 50-ml syringe, which is used to draw in smoke from the cigarette from the other direction. By turning the three-way valve, smoke was drawn from the cigarette to the 50-ml syringe and then released/bubbled slowly into the conical tube containing the medium. The cycle was repeated until the entire cigarette was burned. The resulting solution was filtered using a 0.2-μm filter to remove particulate matter and was referred to as 100% CSE. CSE was prepared freshly for each experiment.

CSE was diluted into RPMI 1640 medium with supplements needed for MLE12 growth for the cell culture experiments. Alternatively, CSE was diluted into the buffer used in the respective reaction: 20 mM sodium phosphate buffer (pH 7.4) for determination of post-translational modification and CD and working solution provided by Enzo (PBE) for the determination of reductase activity of PDI.

Cell Viability—Viability of cells after their exposure to radicals and CSE was assessed by Neutral Red Assay kits as per the manufacturer's instructions (43).

Cell Counting Experiments—4×10^4 cells/ml were seeded into each well of a 24-well plate and let to adhere overnight. The number of cells per well was determined by counting before the addition of CSE and radicals. The cells thereafter were washed and incubated in RPMI 1640 medium with 2% FBS with antibiotics and indicated concentrations of HQ, AC, PN, H_2O_2, and CSE for 30 min, after which the wells were washed twice with PBS; complete culture media were added back, and the cells were counted 24 and 48 h post-exposure.

Protein Preparation—Cells were exposed to the indicated concentrations of the compounds for indicated times, washed twice with PBS, and lysed in lysis buffer containing 50 mM Tris-HCl (pH 7.4), 150 mM NaCl, 1% Triton X-100, and freshly added protease and phosphatase inhibitor cocktails. Lysates were incubated on ice for 30 min and were cleared by centrifugation at 15,000 $\times$ *g* for 10 min at 4 °C. Protein concentrations were determined using Bradford reagent assay (Bio-Rad) with BSA as the standard.

PDI High Molecular Weight Protein Complex (HMWC) Detection—Procedures were performed as described previously (18, 44). Briefly, cells cultured to 75–90% confluence, exposed, and un-exposed were washed twice with ice-cold PBS supplemented with 20 mM *N*-ethylmaleimide, to protect reduced disulfide bonds from further oxidation during lysis, lysed in lysis buffer (20 mM Tris (pH 7.4), 150 mM NaCl, and 0.5% Triton X-100) for 30 min on ice, and cleared by centrifugation. 50 μg of the total protein was separated by non-reducing polyacrylamide gels (no DTT, not boiled). 8% gels were used to detect complexes between PDI and its client proteins.

Western Blot Analysis—Proteins and protein lysates were resolved either at denaturing (for eIF2α and some PDI) or non-reducing conditions (for HMWC, actin, and post-translational modifications). Following electrophoresis, the proteins were transferred onto nitrocellulose membranes (Bio-Rad); nonspecific binding sites were blocked by incubation in 5% nonfat dry milk in Tris-buffered saline (TBS) containing 0.1% Tween 20 (TBS-T) for 1 h at room temperature. For detection of PDI (1:5000) and actin (1:10,000), membranes were incubated for either 2 h at room temperature or overnight at 4 °C in the blocking buffer with indicated primary antibodies. For detection of eIF2α phosphorylation, membranes after blocking were washed twice with TBS-T to remove excess blocking buffer. Membranes were then incubated overnight at 4 °C with primary antibodies against eIF2α-P at a 1:1000 dilution prepared in 5% BSA (bovine serum albumin)/TBS-T solution. After incubation with primary antibodies, all membranes were washed three times in TBS-T for 15 min and then incubated in appropriate secondary antibodies conjugated to horseradish peroxidase for 90 min. Specific proteins were detected using chemiluminescence detection reagents (Denville Scientific or Thermo Pierce). The relative intensity of the bands was determined by densitometric analysis using Quantity One software (Bio-Rad) and was normalized to β-actin.

Mice—C57BL/6 female mice (8–10 weeks old) from Taconic Farms (Germantown, NY) were used for experiments. All mice were housed and used for the experiments under the direction and approved protocols of the Mercer University Institutional Animal Care and Use Committee (protocol A1009016).

CS Exposure in Vivo—C57BL/6 female mice (aged 8–10 weeks) were exposed to either one unfiltered cigarette for acute exposure experiments or to four cigarettes a day for 5 days a week for 6 weeks or 6 months or a sham, using the smoking chamber as described previously (27). Old smokers were exposed to two cigarettes a day for 5 days a week from the age of 1.5 years until 2 years of age.

Tissue Processing for Western Blotting Analysis—Lung and liver tissue homogenates were prepared by homogenizing the tissue in 1 ml of lysis buffer (20 mM Tris (pH 7.4), 150 mM NaCl, and 0.5% Triton X-100) or RIPA buffer (150 mM NaCl, 50 mM Tris (pH 8.0), 2 mM EDTA, 1% Nonidet P-40, and 0.1% SDS) supplemented with a protease inhibitor tablet (Roche Applied Science) and phosphatase inhibitory cocktails 2 and 3 (Sigma). Lysates were cleared by centrifugation and analyzed by gel electrophoresis. Protein concentration was determined using Bradford protein assay (Bio-Rad) with BSA as a standard and verified using a Coomassie Blue gel stain.

Tissue Processing for Immunohistochemistry Analysis—Lungs were inflated by intratracheal instillation of a 10% neutral buffered formalin at 25 cm of H_2O for 10 min. They were then ligated and removed. Inflated lungs were fixed in the formalin solution for 24 h, followed by 48 h of cold PBS wash and paraffin embedding.

Immunohistochemistry—Serial sagittal sections of 4 μm were cut from paraffin-embedded lung slices, placed on silane-coated slides, de-waxed, and rehydrated. Antigen retrieval was done by heating in citrate buffer and blocking of nonspecific binding by incubating in PBS containing 2% normal goat serum. Slides were further incubated with anti-PDI (C81H6) rabbit antibody (1:1000, Cell Signaling catalog no. 3501) diluted in blocking solution overnight and with peroxidase goat anti-rabbit IgG antibody (1:2000, Vector Laboratories, Peterborough, UK, catalog no. PI-100) for 1 h, followed by 3,3′-diaminobenzidine peroxidase (HRP) substrate kit (SK-4100) (Vector Laboratories, catalog no. SK-4100). Images were acquired using EVOS® FL Cell Imaging System (Life Sciences, New York)

PDI Post-translational Modifications—2 μg of recombinant PDI (Enzo Life Sciences) in 20 mM sodium phosphate buffer

(pH 7.4) was treated with 50 μM HQ, 30 μM AC, 40 μM PN, 100 μM H_2O_2, and 10% CSE for 30 min at room temperature, in the presence or absence of 1 mM GSH. Excess compounds were removed by Biospin-6 size exclusion columns (Bio-Rad). Untreated and treated PDI samples were resolved on 10% non-reducing SDS-polyacrylamide gels and analyzed for *S*-nitrosylation of cysteine and tyrosine and for *S*-glutathionylation by the immunoblotting technique. Briefly, nonspecific binding was blocked by incubating membranes for 1 h in blocking buffer (5% nonfat dry milk in TBST). The membranes were than washed three times with TBST for 15 min each time and incubated in the presence of the following primary antibodies diluted in 5% BSA/TBST buffer overnight at 4 °C: anti-glutathione (Virogen Biotech, catalog no. 101-A-100, dilution 1:1000), anti-*S*-nitrosylated cysteine (US Biological, catalog no. C9002-75, dilution 1:500), or anti-nitrotyrosine (US Biological, catalog no. N2700-9, dilution 1:50). The membrane was washed three times with TBTS, incubated with the appropriate secondary antibody diluted in blocking buffer,and washed three times for 15 min each in TBST. The detection was performed using chemiluminescence detection (Denville Scientific).

PDI Spectroscopic Analysis by Circular Dichroism (CD)—Recombinant PDI was treated as described above and analyzed by CD as described previously (19). CD spectra were recorded using Jasco J-815 spectropolarimeter equipped with a Peltier temperature-controlled cell holder and connected to a PC for signal averaging and processing. Changes in the secondary structures of PDI were monitored in the far-UV region (190–250 nm) using 1.0-mm path length quartz cuvette. To reduce the maximum signal to noise ratio, a continuous flow of nitrogen (20 liter/min) was purged to the instrument. All the spectra were collected at 20 °C, and results were expressed in ellipticity units (degrees cm^2 mol^{-1}). Purified wild-type PDI was equilibrated in 20 mM sodium phosphate (pH 7.4) prior to any experiments, and aggregation was removed by centrifugation at 100,000 × *g* for 1 h. The concentration of purified wild-type treated and untreated PDI in the experiments was 50 μg. Data were analyzed using ORIGIN 9 software (OriginLab).

PDI Reductase Activity Assay—Reductase activity of PDI was determined using Proteostat™ PDI assay kit from Enzo Life Sciences. This assay is optimized to identify inhibition of PDI activity and was chosen based on comprehensive review of assays available to measure PDI activity (45). PDI activity was determined according to the manufacturer's instructions (46–49). Briefly, recombinant PDI was incubated with CS radicals (HQ, AC, PN, H_2O_2, or CSE) for 15 min at room temperature in the presence of DTT. Insulin solution was added and incubated for an additional 15 min. The reaction was stopped by the addition of Stop reagent. PDI activity was detected by adding Proteostat™ PDI detection reagent after a 15-min incubation in the dark. The fluorescence was read using FlexStation3 microplate reader at excitation of 500 nm and emission of 603 nm. Bacitracin supplied with the kit was used as a known inhibitor of PDI activity. A Student's *t* test was used to compare differences in PDI enzymatic activity. Means and standard deviations of enzyme activities were quantitated in triplicate and were tested for significance via one-way analysis of variance.

PDI Activity Assay—PDI activity assay was by modification of Gilbert *et al.* (50). Briefly, denatured and reduced RNase A (DrRNase) (made fresh for each experiment) was prepared from native RNase (Sigma, R6513) by incubating 5 mg of native RNase overnight in 1 ml of 0.1 M Tris acetate (pH 8.0), 2 mM EDTA, 6 M in guanidine hydrochloride, and 0.14 M DTT. Immediately before use, the excess of DTT and guanidine hydrochloride was removed using two consecutive filtrations through a Bio-Spin 6 column.

DrRNase was reactivated by co-incubation of 1 μg of PDI (untreated or pre-treated by CS radicals (HQ, AC, PN, H_2O_2, or CSE) as described above) with 15 μg of denatured and reduced RNase in a total volume of 100 μl in 50 mM sodium phosphate buffer (pH 7.5), containing 5 mM EDTA, 1 mM GSH, 0.2 mM GSSG, for 15 min at room temperature. RNase A reactivation was assayed quantitatively upon addition of its substrate cCMP in 50 mM Tris-HCl buffer (pH 7.5), containing 25 mM potassium chloride and 5 mM magnesium chloride (200 μl to obtain total volume of 300 μl), by monitoring the absorbance increase at 286 nm reading every 30 s for 90 min at 25 °C due to the hydrolysis of cCMP by SpectraMax® i3x (Molecular Device, Sunnyvale, CA). PDI activity was expressed as ΔA_{260}/min/mg protein and calculated by maximum linear rate at the first 10 min of the curve using activity of RNase = $(A_{286\,(10\,min)} - A_{286\,(1\,min)})$ (time (9 min) × concentration of protein (mg/ml) × volume of reaction (0.3 ml)). Relative RNase activity restored by untreated PDI is considered as 100%.

Sulfenic Acid Detection—Sulfenic acid detection was performed as described as described by Wani *et al.* (51), by adding the Cys-sulfenic acid interacting compound (DCP-Bio1) directly to the lysis buffer. This prevents any thiol redox reaction during the procedure to influence the redox states of the cysteines. The lysis reaction differs slightly for cells and for tissues. After lysis, which ensures "preservation" of Cys-sulfenic acid as it was in the cells/tissues at the moment of the collection, the sulfenilated proteins were pulled out by biotin tag and added to the Cys-sulfenic acid-binding compound DCP-Bio1.

Lysis of Cells for Sulfenic Acid Detection—Briefly, MLE 12 cells were cultured to 75–90% confluence and incubated with or without CS radicals for the indicated time periods. Cells were washed in ice-cold PBS supplemented with *N*-ethylmaleimide and lysed in ice-cold lysis buffer (50 mM HEPES, 50 mM NaCl, 1 mM EDTA, 1 mM EGTA, 10% glycerol, 1% Triton X-100 with protease inhibitor tablet and phosphatase inhibitor mixtures, 200 units of catalase enzyme, and 200 μM DCP-Bio1(a dimedone-based compound with a cleavable biotin tag, which specifically binds to sulfenilated cysteines) for 1 h on ice. The lysate was spun at 15,000 × *g* for 10 min, and the supernatant was saved as whole cell lysate. Bradford assay was used to estimate the protein concentration.

Tissue Processing for Sulfenic Acid Detection—Lung tissue homogenates were prepared by homogenizing the tissue in lysis buffer (50 mM HEPES, 50 mM NaCl, 1 mM EDTA, 1 mM EGTA, 10% glycerol, 1% Triton X-100 with protease inhibitor tablet and phosphatase inhibitor mixtures, 200 units of catalase enzyme, and 200 μM DCP-Bio1) and passed through a 1-ml tuberculin syringe and incubated for 1 h on ice. The lysates were

spun at 15,000 × *g* for 10 min, and the protein concentration in the supernatant was determined by Bradford assay.

Pulldown to Detect Sulfenilated Proteins—Cell lysates/homogenates (250 μg) were incubated overnight at 4 °C with streptavidin-conjugated agarose beads (Thermo Pierce). The beads were washed twice (50 mM HEPES, 50 mM NaCl, 1 mM EDTA, 1 mM EGTA, 10% glycerol, 1% Triton X-100), and the sulfenilated proteins retained on the beads were boiled with 5× non-reducing Sample buffer, resolved by SDS-PAGE, and analyzed by immunoblotting using anti-PDI antibody.

Statistical Analysis—To calculate standard deviations for Western blot bands, densitometric numbers, obtained using of the Bio-Rad's Quantity-One software, were exported to Excel. The intensity of the bands of interest was normalized to the intensity of the corresponding actin bands for at least three independent experiments for each parameter; and the standard deviation was calculated using the "stdev" function in the program. Statistical significance between the groups (*p* value) was calculated using Student's *t* test formula, which is also built into Excel.

Results

CS Affects ER through Oxidative Damage—We previously demonstrated that CS induces UPR in the lungs of one-time smokers and found that exposure of mouse lung epithelial (MLE12) cells to CSE reflects *in vivo* findings in the total lung. Using MLE12 cells, we demonstrated that UPR induction is due to oxidative damage from CS (18). To identify specific components of CS responsible for the UPR induction, we tested different oxidants present in CS for their ability to cause phosphorylation of eukaryotic initiation factor (eIF) 2α, the immediate downstream target of UPR sensor, PERK, in MLE12 cells. Four major CS radicals were tested, two most common radicals from the vapor phase, PN and H_2O_2, and two long lived radicals from the tar phase, AC and HQ. MLE12 cells were either exposed or not to the indicated concentrations of CSE, AC, HQ, H_2O_2, and PN for different times. The chosen concentrations were previously reported in the literature to mimic smoke exposure (35, 52–54). Exposure to all tested radicals was able to induce phosphorylation of eIF2α (Fig. 1, *A–E*). Exposure to AC and HQ showed strong effect with low variability, whereas exposure to PN and H_2O_2 required higher concentrations to see the effects and was more variable, attesting perhaps to the short lived nature of these radicals (Fig. 1*G*). NAC, a cell-permeable analog of the anti-oxidant glutathione, prevented induction of UPR in response to AC and HQ (Fig. 1*F*).

Neutral Red assay was employed to ensure that the applied concentrations of the radicals did not impair cell viability (Fig. 1*H*). Moreover, recovery assay demonstrated that the tested concentrations of HQ and AC have similar effects on cellular growth dynamics and recovery (Fig. 1*I*). Cells exposed to the indicated concentrations of CSE, HQ, and AC grew very little during the first 24-h post-exposure and resumed normal growth in the following 24 h. PN and a higher concentration of peroxide somehow had a more profound effect on the time when cells were able to resume their divisions. In conclusion, radicals present in CS contributed to UPR induction.

Smoke and Age-related Changes in PDI Levels in Mouse Smokers—We have demonstrated previously that CS exposure leads to the oxidation of one of the main ER-resident chaperones, PDI, in cells and in the lungs of one-time mouse smokers. PDI oxidation by CS radicals can be a major causative agent in induction of UPR (18). It has been reported that PDI protein is up-regulated in human non-COPD smokers, presumably as a protective mechanism to improve the protein folding capacity of the ER affected by smoke (10). We therefore first investigated whether the correlation exists between contingency of smoking and amounts of PDI in the murine model of acute and chronic exposure to cigarette smoke.

We tested the up-regulation of PDI at the levels of mRNA (PDI1a) and protein in total lung lysates, as well as PDI concentrations and distribution in lung sections of mice of different age groups exposed or not to CS for different time periods, namely in one-time smokers (12, 24, and 48 h post-exposure), in young smokers who smoked for 6 weeks (8–10 weeks of age until 14–16 weeks), and in adult and old chronic smokers who smoked for 6 months (ages 8–10 months and 2 years old at the time of analysis, respectively). Fig. 2, *A, D, G,* and *J,* demonstrates that there is no up-regulation of PDI mRNA at any time following exposure to CS. PDI protein up-regulation was not detected in one-time smokers at any time following the CS exposure (Fig. 2, *B* and *C*). The increase in the levels of PDI protein can be clearly detected in total lungs and in the lung sections in young 6-week-old chronic smokers (Fig. 2, *E* and *F*), as well as in 8-month-old and 2-year-old mice exposed to smoke for 6 months. Immunohistochemical staining for PDI demonstrated a strong increase in the amount of PDI protein in epithelial cells in the lining of small airways, where the most extensive CS exposure occurs, and in the cells forming alveolar units (Fig. 2, *F, I,* and *L*). Please note, in the lungs of older mice, a reliable and statistically significant increase can be detected only in the lung sections, attesting that protective adaptation related to the increase in PDI protein is more efficient at a younger age (Fig. 2, compare *I* to *L*). We concluded that our murine model of COPD mimics PDI up-regulation detected in humans smokers, which was also detected at the level of the protein (10, 55). We found that this increase in the protein levels is the most prominent in young smokers and slowly declines with age.

CS Oxidizes PDI in Vivo in Mouse Smokers—PDI has four cysteine residues in its conserved thioredoxin-like catalytic domains. Sulfenilation (–SOH) is a well established first intermediate in the oxidation of cysteine residues (56, 57), and due to immediate preservation of cysteines, the redox state during lysate preparation can be reliably detected in tissue samples. Knowing that CS indices UPR through oxidative damage, we tested whether CS preferentially inactivates cysteine residues within PDI in mice exposed to CS. To detect cysteine sulfenic acid (Cys-SOH) formation, lysates were prepared from fresh whole lungs with the sulfenic group interacting agent DCP conjugated to biotin added to the lysis buffer, followed by PDI immunoprecipitation. Fig. 3*A*, *left panel* demonstrates that exposure to CS causes extensive sulfenilation of PDI in mice lungs, even after exposure to one cigarette.

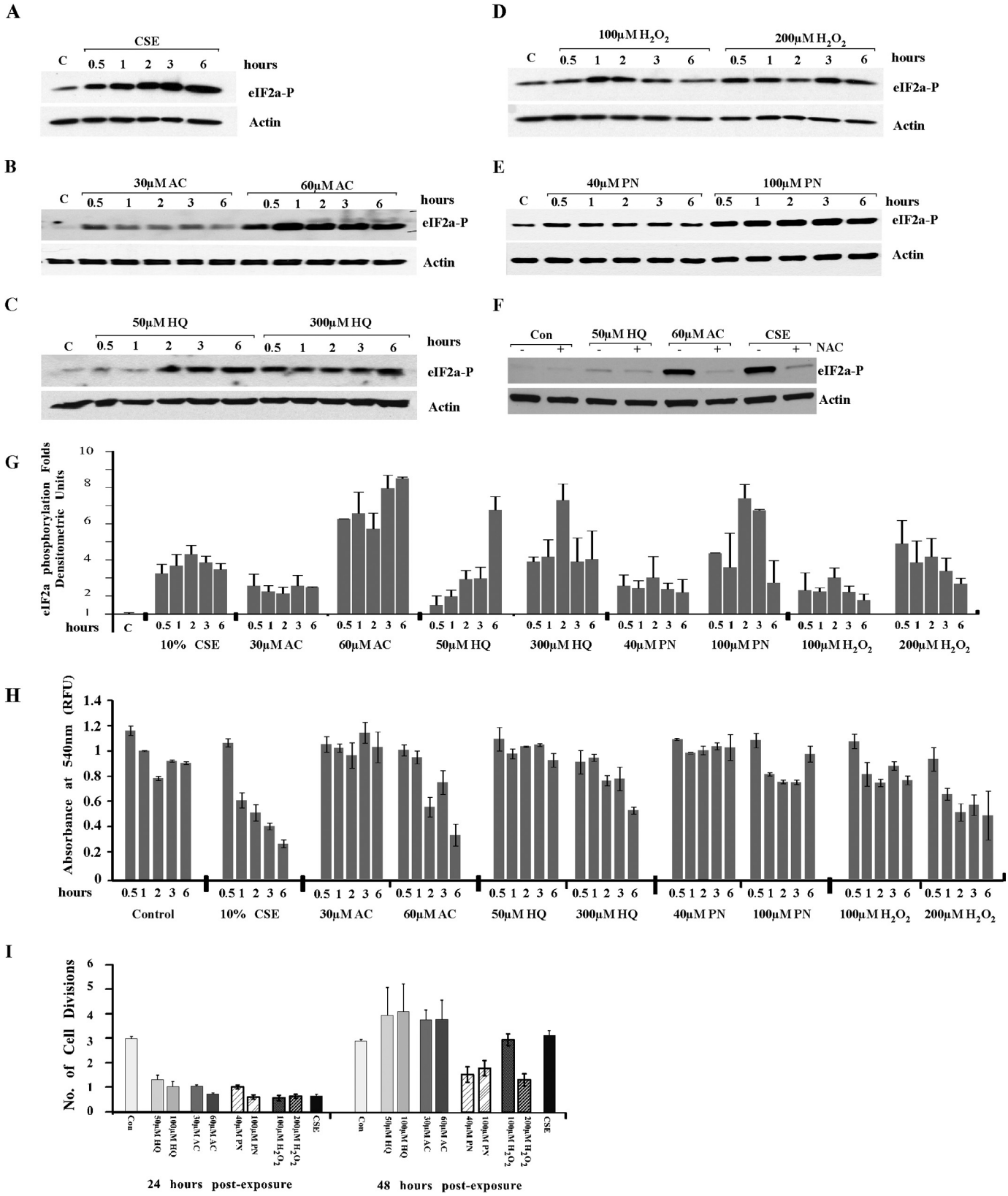

FIGURE 1. **Radicals present in CS are responsible for UPR induction.** MLE12 cells were exposed or not to the indicated concentrations of CSE (*A*), AC (*B*), HQ (*C*), H_2O_2 (*D*), and PN (*E*) for the indicated times. *F*, in indicated experiments AC, HQ, and CSE were added together with NAC. By the end of the incubation, cells were lysed, and lysates were checked for the presence of the phosphorylated form of eIF2α. Actin was used as a loading control (*Con*). Gels are representative from at least three repetitive experiments. *G*, graph represents quantitation of eIF2α phosphorylation. *H*, cell viability by the end of the exposure time was tested using a Neutral Red kit. *I*, MLE12 cells were exposed or not to HQ, AC, PN, H_2O_2, and 10% CS extract for 30 min, washed twice, and allowed to recover for indicated periods of time. Cells were counted by the end of indicated recovery times.

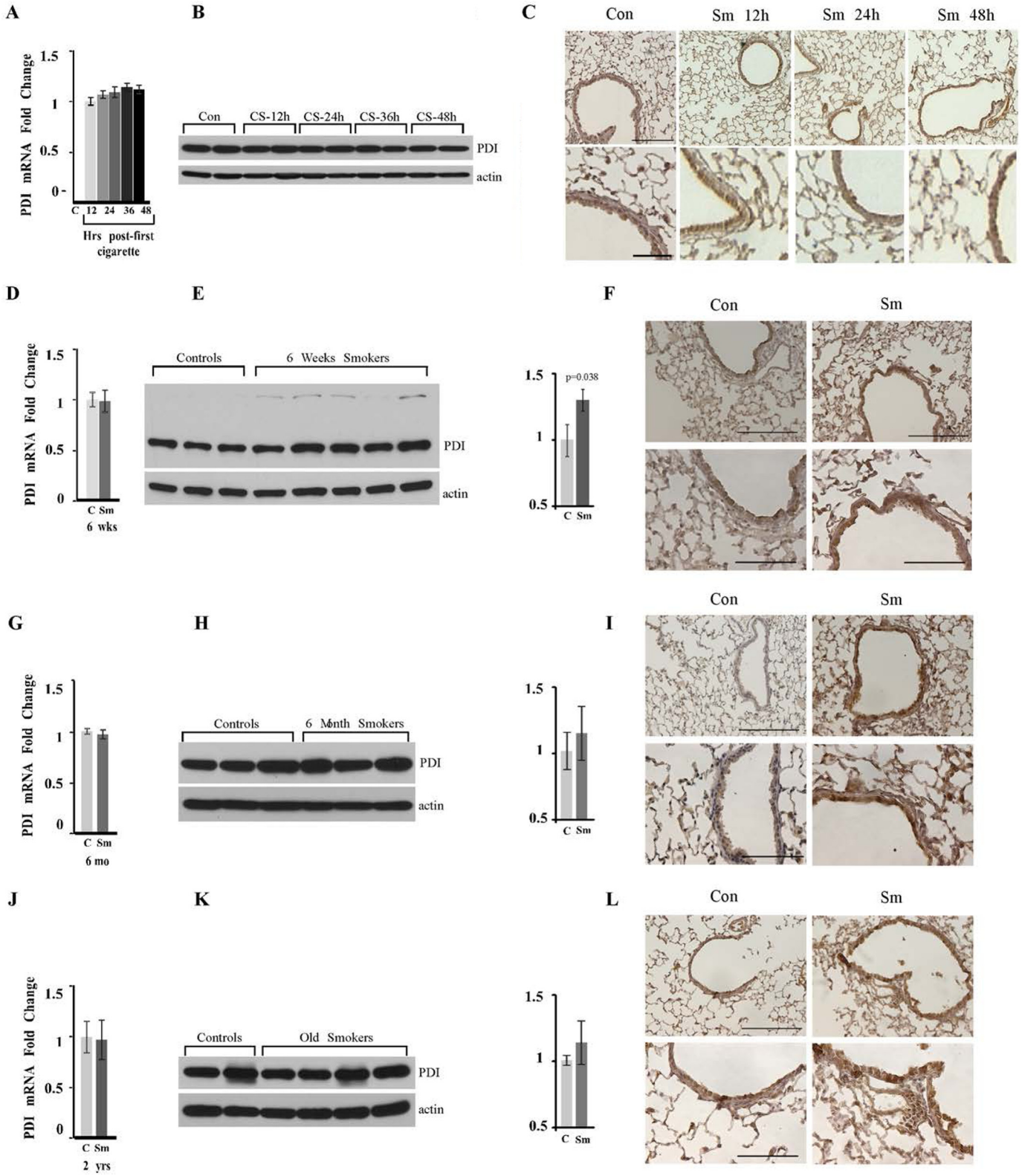

FIGURE 2. **PDI protein is up-regulated in murine smokers.** Wild-type C57Bl/6 mice were exposed or not to CS for the indicated periods of times. Lungs were harvested and lysed. Exposure periods are one-time smokers (*A–C*); 6-week chronic smokers (*D–F*); 8-month-old chronic smokers, exposed for 6 months (*G–I*), and 2-year-old chronic smokers, exposed for 6 months (*J–L*). Amount and distribution of PDI mRNA (*A, D, G,* and *J*) and PDI protein (*B, E, H,* and *K*) were determined in total lung lysates of control (marked as *C* or *Con*) and smoke-exposed (marker as *Sm*) animals by quantitative RT-PCR and Western blotting analysis. The *graph* on the *right* represents quantitation of the amounts of PDI protein by densitometry units ($p = 0.038$ for 6-week smokers; $p = 0.2601$ for 8-month smokers; and $p = 0.2064$ for old smokers). Actin was used as loading control. *C, F, I,* and *J,* lungs of age-matched controls (*right panels*) and smokers (*left panels*) were stained as one set using identical conditions with anti-PDI antibody. *Upper panels* images acquired at ×200 magnification. *Lower panels* images represent enlarged areas from original images acquired at ×400 magnification. *Scale bars,* 100 μm for the *upper panels* and 200 μm for the *lower panels*. Images are representative of at least three animals analyzed for each group.

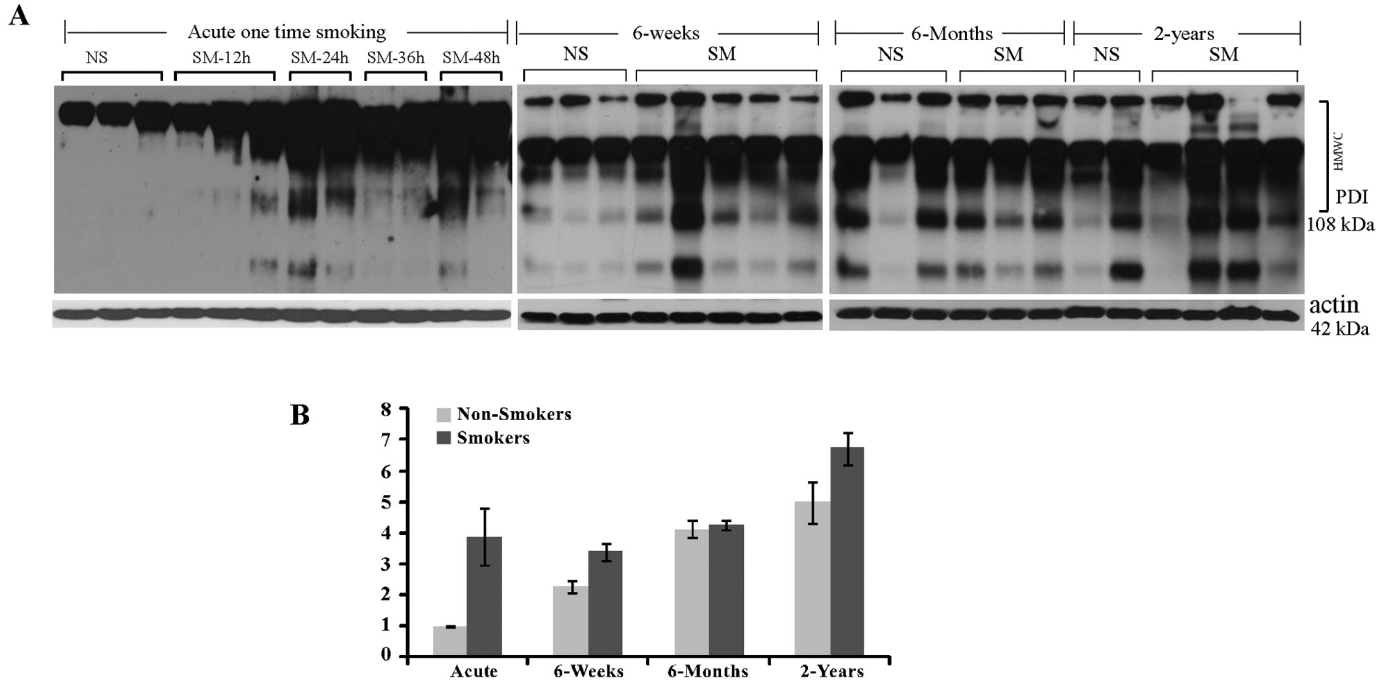

FIGURE 3. **PDI protein is heavily sulfenilated in the lungs of murine smokers.** *A,* lungs of one-time smoker mice at different times post-exposure and lungs of chronic smokers exposed to smoke at different ages were harvested, and sulfenilated proteins were immunoprecipitated from total lung lysates and separated at non-reducing conditions. Western blots were probed for the presence of PDI among sulfenilated protein. Please note that sulfenilated PDI was observed to be predominantly present in HMWCs, which contain protein complexes with size over 108 kDa. *B, graph* represents quantification of sulfenilated PDI in controls and smokers of different ages. Relative quantitation of one-time and age-matched controls was performed by running one of acute controls and one of acute smokers on each gel.

We compared the amounts of oxidized PDI in acute and chronic mouse smokers and their age-matched controls. We determined that the levels of sulfenilated PDI gradually increase with age in smoker mice and to a much lesser extent in their age-matched non-smoker controls (Fig. 3), making the oxidation of PDI potentially relevant to aging in general and to the age of COPD onset particularly.

CS Effects on PDI Are Mediated through PDI Thiols and Tyrosine Oxidation—The precise mechanism by which CS radicals cause PDI oxidation is not known. *In vivo* sulfenilation data suggest that post-translational modifications of cysteines are one of the possible mechanisms. We used recombinant PDI protein to further our understanding of post-translational modification inflicted by CS radicals. Recombinant PDI was pre-treated with the indicated concentrations of HQ, AC, PN, H_2O_2, or CSE for 30 min, resolved on non-reducing SDS-PAGE, and probed for the presence of post-translational modifications on cysteines and tyrosines, both of which are conserved in two thioredoxin-like domains of PDI, a and a′, which form the active center responsible for enzymatic activity (Fig. 4). Exposure to AC and CS resulted in cysteine *S*-nitrosylation probably as an intermediate reaction in formation of PDI-acrolein-aldehyde adducts (Fig. 4*A*). Exposure to PN caused nitration and conjugation of nitric oxide to oxidized tyrosine residues (Fig. 4, *B* and *C*). Therefore, CS caused post-translational modifications of the residues important for three-dimensional structure and activity of PDI.

CS-induced Post-translational Oxidation Affects Structure of PDI—To test the hypothesis that radicals from CS alter secondary structure of PDI we used circular dichroism (CD), a technique used to monitor the extent of conformational changes (58, 59). The thioredoxin-like domains of PDI were found to be spatially organized in the shape of twisted U as was shown previously (23), where the CD spectra of native PDI show the presence of $n \rightarrow \pi^*$ transition centered around 222 nm and $\pi \rightarrow \pi^*$ transition around 208 nm, which is a characteristic of structured α-helices (Fig. 5*A*, *red trace*). Incubation of PDI with AC or HQ resulted in significantly decreased ellipticity and major loss of helical content of the protein, with HQ having a more prominent effect on the α-helix (Fig. 5, *A–C*). Incubation of PDI with PN caused a maximal decrease in the β-sheet region and an increase in coil (Fig. 5, *A* and *E*), where incubation with H_2O_2 mildly affected the β-sheet with a minimally changed α-helix (Fig. 5, *A* and *D*). These results indicate that the contact of PDI with radicals from CS leads to structural changes in the protein, mainly to protein unfolding due to the formation of more random coil structure.

PDI has been shown previously to be *S*-glutathionylated during different physiological oxidative stresses and in some disorders (19). ER lumen is a highly oxidized environment with a limited amount of reduced glutathione (ratio of GSH to GSSG is 1:1 in ER and 100:1 in the cytosol). Nevertheless, GSH is used as a reducing agent in multiple reactions in the ER. We therefore tested how the presence of glutathione affects the PDI structural changes caused by CS radicals. The CD spectra (Fig. 5, *F–H*) demonstrated no change in ellipticity when GSH was added together with AC and HQ. Thus, GSH may protect PDI from AC- and HQ-induced oxidation by titrating those compounds away from PDI in a possible reaction depicted in Fig. 4*C*. Addition of H_2O_2 together with glutathione resulted in a

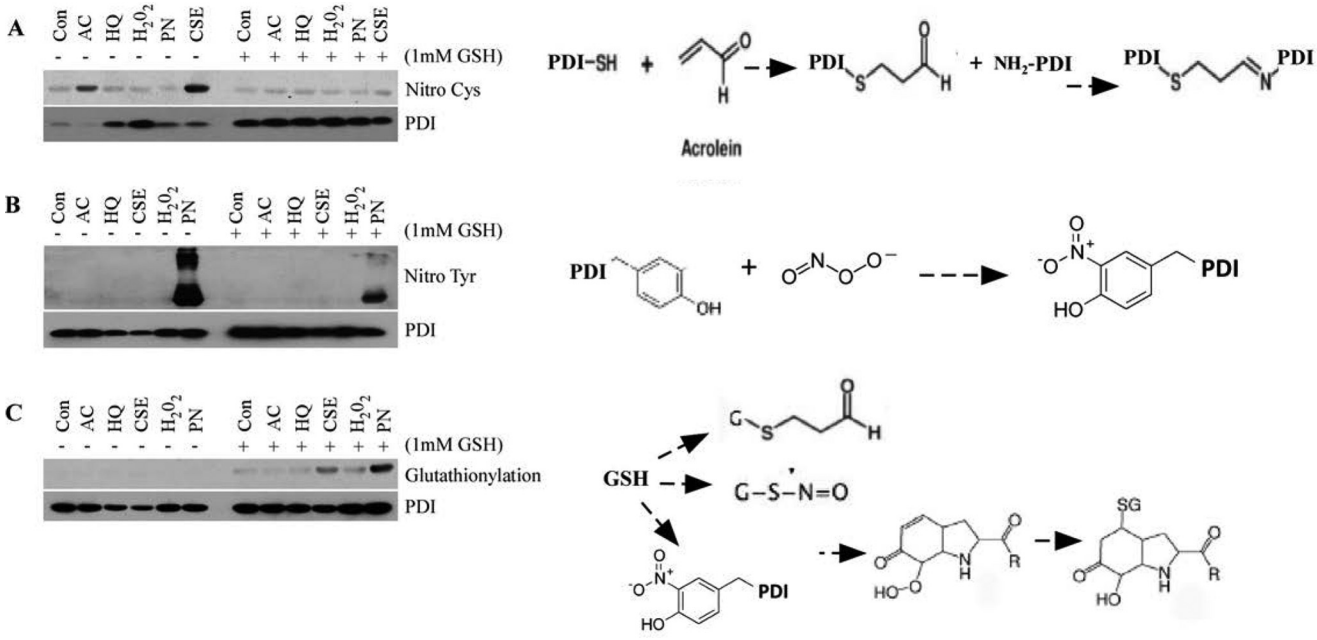

FIGURE 4. **CS exposure of PDI results in cysteine and tyrosine oxidative modifications.** Recombinant PDI was treated or not with indicated concentrations of HQ, AC, PN, H_2O_2, or CSE for 15 min and analyzed for nitrosylation of cysteines (*A*), tyrosines (*B*), and glutathionylation (*C*). *Right panels* depict hypothetically predicted schematic reaction of PDI modifications.

small but consistent increase in the α-helix content of the protein (Fig. 5*I*), although addition of PN led to a major shift in the α-helical contents and random coil structure (Fig. 5*J*). Moreover, our results from Fig. 4*C* indicate that exposure to PN may cause *S*-glutathionylation of PDI. This modification has been shown to affect PDI activity, is usually reversible, and prevents further oxidative damage to the protein (see under "Discussion"). Therefore, CD data correlates well with our findings presented in Fig. 4.

Changes in PDI Structure Resulted in Inhibition of PDI Enzymatic Activity Both in Vitro and in Vivo—PDI is a conformation-sensitive protein; changes in its secondary and three-dimensional structure can affect its enzymatic activity. To test this, we measured PDI activity following exposure to CS radicals *in vitro* and *in vivo*. *In vitro* oxidoreductase activity of PDI exposed to radicals from CS was measured as the ability of PDI to reduce its well described substrate insulin (Fig. 6*A*). These results are consistent with the changes in three-dimensional structure of PDI that we found after exposure to AC, HQ, and PN (Fig. 5, *A*–*C*). Changes induced by exposure were mild and differ from the changes inflicted by other radicals. The effect of H_2O_2 also agrees with the previously described role of H_2O_2 in assisting in disulfide bond formation (38, 39).

PDI activity was measured *in vitro* by its ability to assist in folding of denatured and reduced RNase. RNase activity recovery in the presence of PDI is measured by hydrolysis of its substrate cyclic cytidine monophosphate (cCMP) (50). Fig. 6*B* demonstrated that exposure of PDI to the lowest tested concentration of CSE and radicals presented in it leads to a significant lag in RNase reactivation. The untreated RNase activity was calculated to be 0.0023/min/mg of protein. It was further used to calculate relative RNase A activity by comparing the rates of increase in RNase A activity during the linear phase. We found that exposed PDI possesses only 40% of the activity of that of non-exposed protein (Fig. 6*C*).

The ability to induce formation of PDI-containing High Molecular Weight Complexes (HMWC) in exposed cells was used to test PDI activity *in vivo*. HMWC are short lived intermediates in protein folding that can be detected on non-reducing gel along with free PDI. They contain PDI-client protein complexes. Normally, these complexes will be resolved as proteins mature, and their persistence indicates PDI's inability to form disulfide bonds and the non-maturation of PDI client proteins (18, 60). Exposure to tar phase radicals of cigarette smoke, AC and HQ, resulted in robust induction of HMWC at any concentration tested (Fig. 6*D*). Short lived PN did not induce HMWC at the lower concentrations tested presumably due to their inability to reach and enter the ER compartment. Nevertheless, high concentrations of PN act as strong inducers of PDI-HMWC (Fig. 6*D*). H_2O_2 has very little effect on the formation of HMWC (Fig. 6, *D* and *E*). All radicals that induced extensive HMWC also resulted in the formation of boiling and reduction-resistant adducts between PDI and its client protein (Fig. 6*E*).

Therefore, long lived radicals of the tar phase of CS were able to reach the ER and lead to the oxidation of the ER-resident PDI and compromise protein folding. In addition, short lived PN radicals can cause oxidation of the cytosolic and plasma membrane pools of PDI and may cause oxidation of ER-resident PDI at very high concentrations.

Discussion

Exposure to CSE and the radicals present in it leads to activation of UPR. We identified a specific molecular mechanism by which CS exposure can induce UPR as follows: oxidation of a PDI, an ER-resident redox-sensitive chaperone responsible for disulfide bond formation.

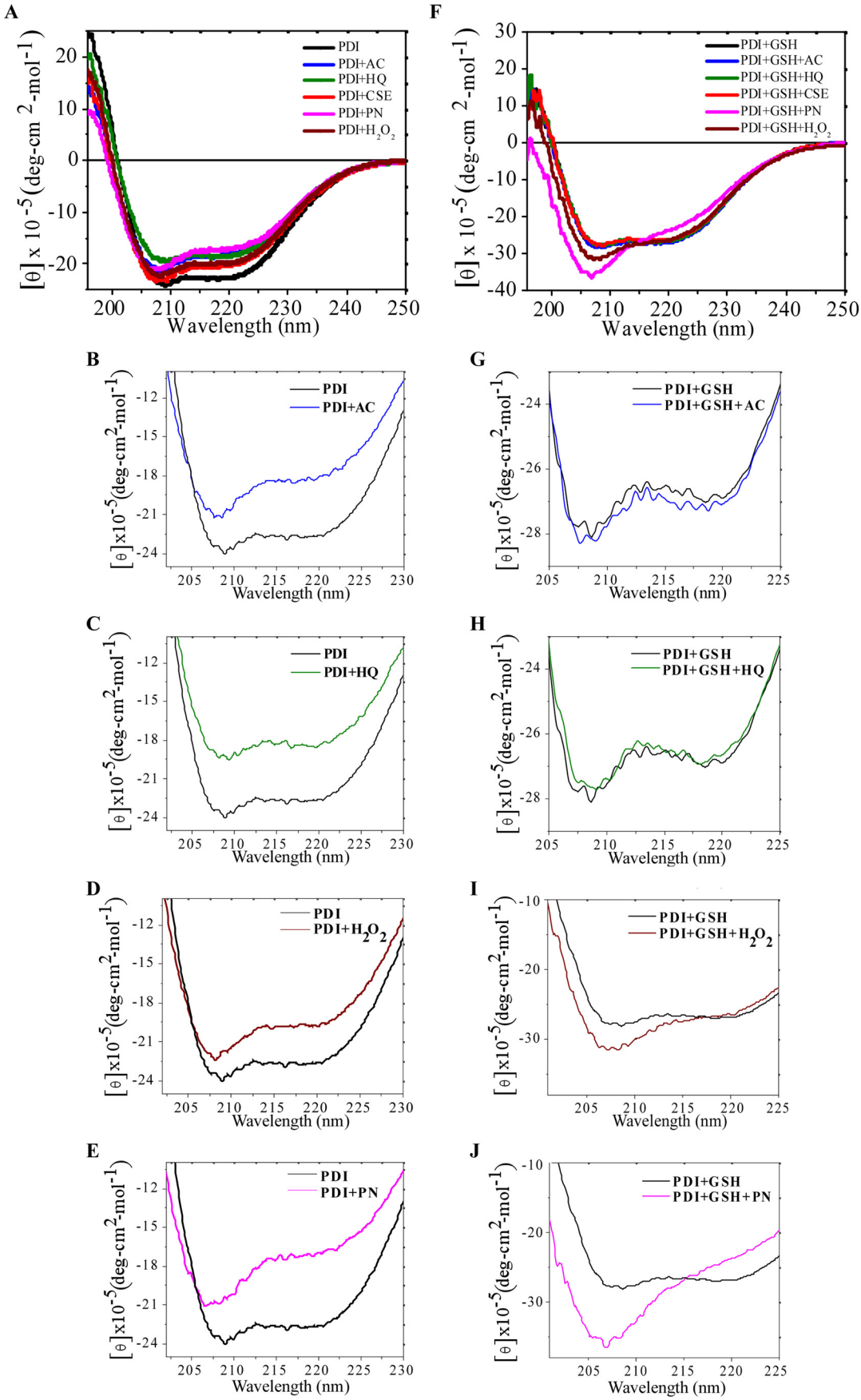
A
PDI
PDI+AC
PDI+HQ
PDI+CSE
PDI+PN
PDI+H2O2
[θ] x 10-5(deg-cm 2-mol-1)
Wavelength (nm)
F
PDI+GSH
PDI+GSH+AC
PDI+GSH+HQ
PDI+GSH+CSE
PDI+GSH+PN
PDI+GSH+H2O2
B
PDI
PDI+AC
G
PDI+GSH
PDI+GSH+AC
C
PDI
PDI+HQ
H
PDI+GSH
PDI+GSH+HQ
D
PDI
PDI+H2O2
I
PDI+GSH
PDI+GSH+H2O2
E
PDI
PDI+PN
J
PDI+GSH
PDI+GSH+PN
[θ]x10-5(deg-cm2-mol-1)
Wavelength (nm)

We concentrated on PDI as a starting point in delineation and understanding of the implications of the redox changes inflicted by CS to protein folding in the ER. PDI is a very abundant protein, one of the main ER-resident chaperones present at the concentration of above 400 μM in the ER lumen (45), where it ensures proper disulfide bond formation and by doing so the acquisition of the correct secondary structure by newly synthesized proteins (24). PDI is also known to localize to other membrane compartments in cells and to be secreted. Disturbance in the PDI can have a more prominent effect than disturbance in less abundant family members, which will be the topic of future research. Moreover, modified PDI in some systems becomes pro-apoptotic, and its presence leads to cell loss (19, 20, 28, 29, 61), the feature characteristics of COPD (5, 62–64).

We demonstrated that PDI, in CS-exposed cells and tissues, loses its enzymatic activity due to oxidation of cysteines and tyrosines in its catalytically active center. We showed that long lived radicals of cigarette smoke, such as acrolein and hydroxyquinones, are able to reach the ER and are most probably responsible for oxidation of ER-resident PDI, although short lived peroxynitrites may be responsible for the oxidation of membrane and cytosolic pools of PDI. The amount of oxidized PDI in lung tissues is proportional to age and smoke exposure. Therefore, CS exposure may result in the situation analogous to premature aging where the decline of chaperones is one of the hallmark of the aging process.

PDI levels have been found to be elevated in the lungs of human "healthy" non-COPD smokers (10). We studied the dynamics of changes in PDI expression levels in young mice from initial exposure to CS until chronic exposure in elderly mice. No changes in PDI mRNA levels were observed between controls and smokers in total lung lysates at any time during CS exposure. PDI protein up-regulation was undetectable in one-time smokers at any time tested following exposure to one cigarette. An increase in PDI protein was detected 6 weeks after initiation of smoking in total lung lysates, although murine smokers are young and their ER is adjusting well to CS challenge with no visible air-space enlargement (COPD), correlating well with what was found in "healthy" non-COPD human smokers. Levels of PDI protein in total lung lysates were variable among older controls and age-matched chronic smokers with detectable air-space enlargement. Nevertheless, the increase in the levels of PDI was most prominent when analyzed in lung sections and was found in epithelial cells of the lining of the airways, where direct exposure to CS vapors occurs (Fig. 2). Increase in the levels of PDI protein should have a protective effect, aiding in adapting function in the presence of reactive oxygen species. The protective role of high levels of PDI was previously shown in some systems, including some neurodegenerative disorders and cancer (40, 65).

The precise mechanism that leads to an increase in the levels of PDI protein is not clear. It can potentially come from either regulation at the level of translation of the protein or from lower protein turnover. Indeed, measurement of relative levels of mRNA, which did not change for PDI1 in smokers, does not account for translational efficiency, which is a mechanism for the regulation of protein production in cells (66–68). One possibility is that there is controlled differential loading of ribosomes onto PDI1 mRNA in young smokers. Indeed, translational regulation that involves differential loading of ribosomes onto mRNAs emerge lately as a mechanism used by effectors of endoplasmic reticulum stress response (69). For example, during host invasion by the pathogenic fungus *Aspergillus fumigatus*, the fungus experiences ER stress, which results in limited remodeling of fungal translatome leading to up-regulation of mRNA-encoded proteins involved in translation, whereas other proteins are differentially loaded into ribosomes. This response was suggested to support adaptive stress-response pathways to support host survival in hostile and stressful environments (70). Reported translational regulation was suggested to provide the cell with a mechanism to fine-tune levels of proteins important for resistance to an environmental stress situation that may be similar in this regard to exposure to CS.

The other possibility to account for the higher levels of PDI protein in smokers is lower protein turnover. PDI is a long lived protein with a half-life of at least 96 h (71), and therefore further stabilization of unmodified functional protein is less likely. PDI however is modified by CS (see under "Results" and below) and modified non-functional PDI is expected to be cleared from cells. Current knowledge about proteasomal degradation in smokers demonstrated that its efficiency declines due to smoke exposure and age (72, 73). The prediction would be that PDI degradation declines with age, and therefore, as smokers age, more modified PDI will persist in lung cells. We detected higher protein levels in young but not older smokers; therefore, if the lower turnover of PDI is the reason for higher protein levels, then it is not clear why lower turnover is not observed in old smokers. Nevertheless, it may represent a novel adaptation-related mechanism to maintain higher protein levels, of which we are currently unaware.

We found that CS exposure leads not only to PDI up-regulation but also to its oxidation (18) and extensive sulfenilation in the lungs of smokers. We demonstrated previously that low pK_a cysteine residues of the PDI active center are primary targets for post-translational modification and inactivation during oxidative and nitrosative stress conditions (19). The sulfenic acid formation is the first intermediate in the oxidation of those cysteines (56), and we demonstrated that cysteines within PDI thioredoxin domains, which are reactive (low pK_a) cysteine residues, themselves are oxidized in cells and animals exposed to CS (18). This initial oxidation can proceed to the modifications such as conversion of sulfenic acid to sulfinic and irreversible sulfonic acids, respectively (26, 56). Those reactions are mediated directly by radicals and do not require additional enzymes. Because some of PDI becomes insoluble and trapped within boiling and reduction-resistant HMWCs, it is possible that the smoke-exposed ER microenvironment may stabilize the cysteine sulfenic acid and make it sensitive to hyperoxidation to

FIGURE 5. **CS-induced post-translational oxidation affects three-dimensional structure of PDI.** Recombinant PDI was treated or not with indicated concentrations of HQ, AC, PN, H_2O_2, or CSE for 30 min without (*A–E*) or with addition of glutathione (*F–J*). Structure of treated and untreated PDI was analyzed using circular dichroism.

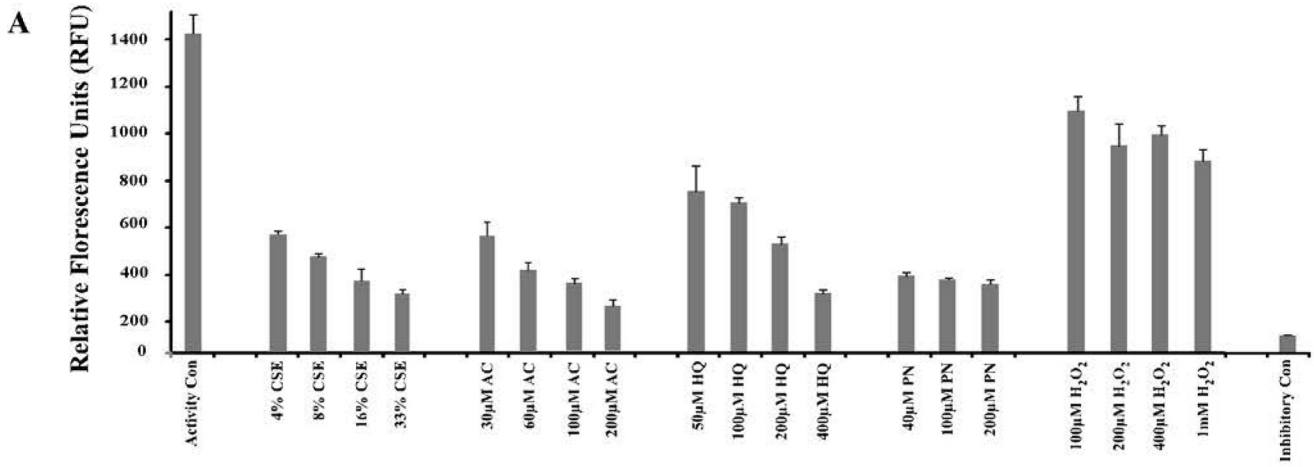
A
Relative Florescence Units (RFU)
1400
1200
1000
800
600
400
200
0
Activity Con
4% CSE
8% CSE
16% CSE
33% CSE
30μM AC
60μM AC
100μM AC
200μM AC
50μM HQ
100μM HQ
200μM HQ
400μM HQ
40μM PN
100μM PN
200μM PN
100μM H_2O_2
200μM H_2O_2
400μM H_2O_2
1mM H_2O_2
Inhibitory Con

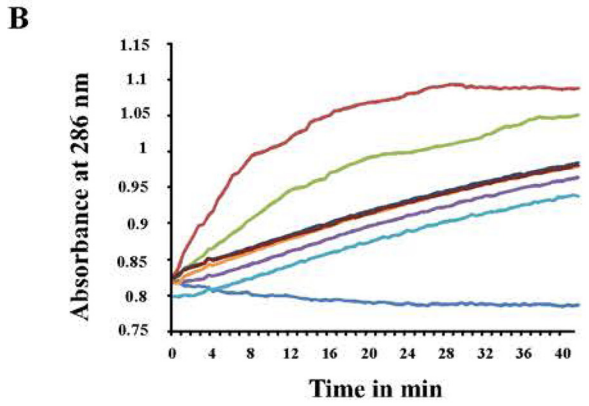
B
Absorbance at 286 nm
1.15
1.1
1.05
1
0.95
0.9
0.85
0.8
0.75
0 4 8 12 16 20 24 28 32 36 40
Time in min

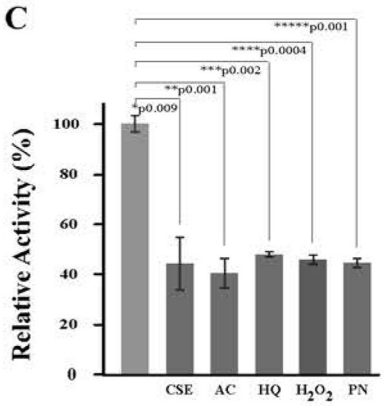
C
*****p0.001
****p0.0004
***p0.002
**p0.001
*p0.009
Relative Activity (%)
100
80
60
40
20
0
CSE AC HQ H_2O_2 PN

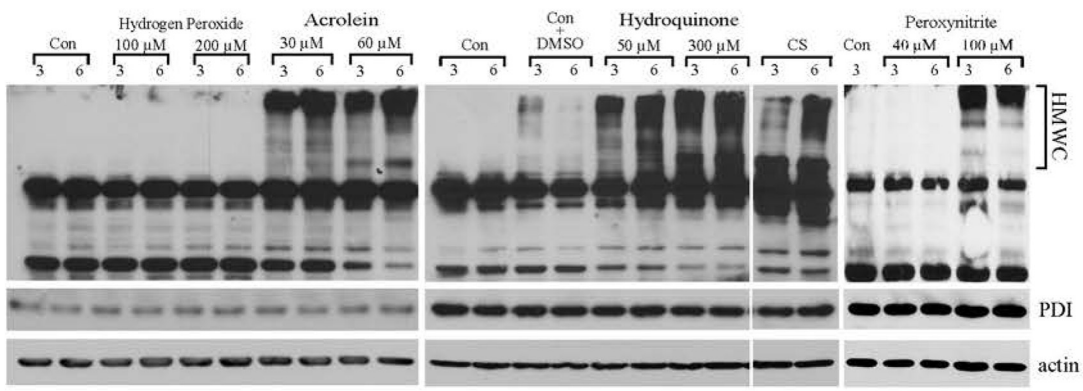
D
Hydrogen Peroxide
Con
100 μM
200 μM
Acrolein
30 μM
60 μM
Con
Con + DMSO
Hydroquinone
50 μM
300 μM
CS
Con
Peroxynitrite
40 μM
100 μM
3 6
HMWC
PDI
actin

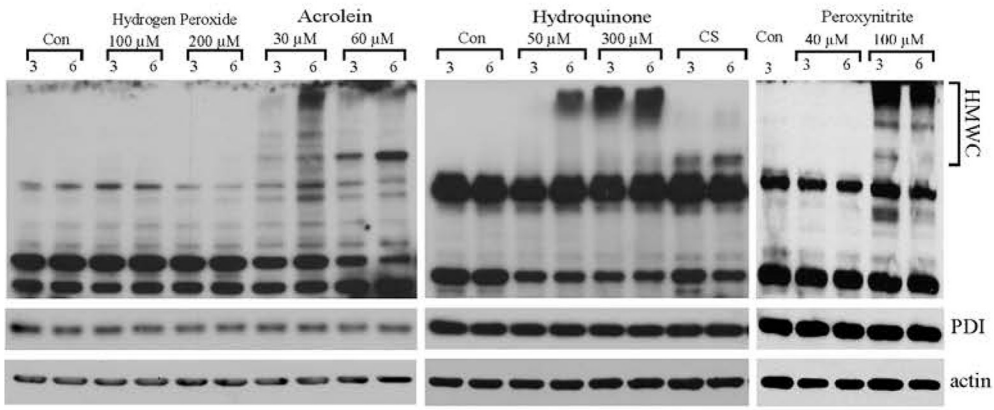
E
Hydrogen Peroxide
Con
100 μM
200 μM
Acrolein
30 μM
60 μM
Con
Hydroquinone
50 μM
300 μM
CS
Con
Peroxynitrite
40 μM
100 μM
3 6
HMWC
PDI
actin

sulfinic and sulfonic acids. At the same time, we detected additional post-translational modification of PDI by acrolein and hydroxyquinones. Whether PDI-sulfonic acid or PDI-acrolein and HQ addicts contribute to irreversibly oxidized fraction of PDI is not known and will be the subject of future research.

Alternatively, sulfenilated cysteines can be further reduced to the thiol state by glutaredoxin, sulfiredoxin, and thioredoxin. We do not have any indication that reduced cysteines of thioredoxin domains of PDI itself can act as sulfenic acid acceptors/reducers from oxidized PDIs or from other client proteins. But this possibility cannot be excluded either. As an alternative mechanism to protect against hyperoxidation, sulfenilated cysteines can be conjugated to glutathione (GSH) by glutathione *S*-transferase (GST) or glutaredoxin. PDI glutathionylation has been reported by us and others and is shown to inactivate PDI enzymatic activity, while protecting it from further oxidation and initiate redox signaling events (19, 20, 28). Polymorphism in different GST alleles is linked to genetic susceptibility for the development of COPD in smokers, as well as to the predisposition of smokers to develop different malignancies, including lung cancer (74–80). Therefore, the possibility exists that some of the effects of different alleles of GST can be the consequences of the "protecting" PDI function from irreversible oxidation.

Those PDI modifications have the potential to blunt and to regulate PDI activity (20, 29, 30). Moreover, we found that the amount of sulfenilated PDI in the lungs increases with the age of mice, and this increase is more robust in smokers. A gradual decline in the efficiency of ER-resident chaperones due to accumulative damage from free radicals has been proposed as one of the reasons for ER aging and is shown to correlate with the onset of proteostasis imbalance-related diseases, where the "young" proteome is able to handle proteins folding efficiently but the aged proteome is failing (81, 82). In CS exposure, the young proteome is able to adjust and re-establish ER homeostasis without eliciting strong pro-apoptotic UPR, whereas the aged proteome is not efficient enough to counter-balance accumulating radicals from CS. Therefore, age-related onset of COPD can at least be partially due to age-related accumulation of oxidized PDI. Indeed, proteostasis imbalance has been reported in COPD and correlates with the severity of the disease (83). PDI is a very abundant redox-sensitive chaperone. Its inactivation by reactive oxygen species can itself be sufficient to lead to premature proteome aging or can reflect the state of the whole proteome (84, 85).

We therefore started to delineate molecular mechanisms of the effect of CS radicals on PDI. We analyzed the effects of the four most common radicals found in CS as follows: two long lived radicals from tar phase, acrolein, and hydroxyquinones; and two short lived radicals from aliquot phase, hydrogen peroxide, and peroxynitrites. Exposure to AC, HQ, and CS resulted in cysteine nitrosylation, sulfenilation, and formation of PDI-acrolein-aldehyde adducts. Those modifications led to the conformational changes in the protein, which were associated with the decline of PDI enzymatic activity *in vitro* and *in vivo*. Indeed, short exposure to low concentrations of CSE resulted in over 60% inhibition of PDI oxidoreductase and 50% isomerase activities. Therefore, CS-exposed cells have to adjust to functioning with suboptimal levels of PDI activity. Noteworthy, oxidized PDI persists in cells for at least 24 h. The reasons for this persistence are under investigation. Those findings strongly support our initial hypothesis that CS exposure results in the situation analogous to premature aging with a decline in efficiency of ER-resident chaperones. Moreover, HMWC between PDI and other proteins were resistant to reduction in cells exposed to AC, HQ, and CS, indicating irreversible PDI modification and formation of stable PDI adducts. It has been shown that cellular toxicity is related to kinetics and stability of adduct formation (86). Their persistence may be critical determinants in the induction of UPR-related pro-apoptotic signaling, especially if they become insoluble and accumulate within the ER (28, 41). Post-translational modifications of PDI have previously been shown to abrogate the protective effect of high levels/up-regulation of PDI. Our results demonstrated that *in vitro*, glutathione rescues PDI from AC- and HQ-induced damage, as determined by rescue of structural changes in PDI and inhibition of UPR induction. Nevertheless, administration of glutathione to smokers had a less protective effect than was expected, possibly due to the complexity of the biological system and bioavailability such that it did not reach the ER in cells experiencing an oxidative challenge (87–89). Therefore, those components of CS are prime suspects in terminal cell toxicity through multiple mechanisms, among which PDI modifica-

FIGURE 6. **Radicals found in CS have inhibitory effect on PDI activity both *in vitro* and *in vivo*.** *A,* recombinant PDI was treated or not with indicated concentrations of HQ, AC, PN, H_2O_2, or CSE for 15 min; insulin was added for an additional 15 min, and by the end of the incubation PDI reductase activity was measured by colorimetric assay, which reflects the amounts of reduced insulin. S.D. were calculated from at least three independent experiments. *B,* recombinant PDI was treated or not with 50 μM HQ, 30 μM AC, 40 μM PN, 100 μM H_2O_2, or 10% CSE for 15 min; DrRNase was co-incubated with treated or not treated PDIs for 30 min. Isomerase activity of PDI was determined by measuring continuously the absorbance increase at 286 nm following addition of RNase substrate cCMP for indicated times. *Brown trace* represents native RNase; *blue trace* represents DrRNase; *green trace* represents DrRNase+PDI; *purple trace* represents DrRNase+PDI+CSE; *cyan trace* represents DrRNase+PDI+AC; *dark red trace* represents DrRNase+PDI+PN; *orange trace* represents DrRNase+PDI+HQ; and *dark blue trace* represents DrRNase+PDI+H_2O_2. *Graph* is representative of three independent experiments. *C,* relative PDI activity, where initial rate of cCMP hydrolysis by RNase was calculated during lag phase (the first 10 min of the curve); relative RNase activity restored by untreated PDI is considered as 100%. Standard deviations were calculated from three independent experiments. Statistical significance between the treated and control groups was calculated using the "Student's *t* test. *D* and *E,* MLE12 cells were exposed or not to PN and H_2O_2,and to tar gases of CS, HQ, and AC for indicated times, lysed, resolved on gel under non-reducing (*D*) or reducing (*E*) conditions, and immunoblotted for the ER chaperone PDI. PDI was found in multiprotein complexes (HMWC) in HQ, AC, and high concentrations PN-treated cells. Significant amounts of HMWC from AC-, HQ-, and PN-treated cells were boiling- and detergent-resistant, attesting to irreversible nature of PDI-acrolein or other adducts. Actin was used as loading control for non-reducing gels. *Middle panels* of *D* and *E* represent additional loading controls, where the same amounts of lysates were resolved on 10% reducing gels and probed for PDI. *Con* represents control cultures. Please note the control with added DMSO was used only as a control for the higher concentration of hydroxyquinones during HMWCs formation and not for the rest of the radicals; those stock solutions were prepared or provided by the company as aliquot solutions. This was included because DMSO has been shown to be cytotoxic (acute and chronic) to the cells if the levels exceed 1% (v/v) (93, 94). Dilution of 10 mM stock solution of HQ in DMSO resulted in 3% DMSO in culture to reach 300 μM HQ (and 0.5% to reach 50 μM HQ). Cells treated with 3% DMSO were therefore used as a control to ascertain that HMWCs are predominantly formed as a result of exposure to 300 μM HQ and not DMSO. Comparison of Control-DMSO and 300 μM HQ HMWCs clearly proves that the changes we are seeing are due to the HQ and not DMSO. Addition of 0.5% DMSO had no effect on HMWC formation (data not shown).

tions and UPR induction may be important; as can be seen in Fig. 3, PDI sulfenilation *in vivo* persists and is not cleared from the cells for a very long time following CS exposure, which may eventually lead to enhanced cellular toxicity.

Exposure to PN resulted in possible tyrosine modification by and possible conjugation of glutathione to oxidized tyrosine residues (Figs. 3 and 4). This was an interesting and intriguing finding, because only recently the possibility of glutathione addition on the tyrosine residues was shown as a possible physiological mechanism for protein *S*-glutathionylation or cross-linking (90). PDI previously was shown to be *S*-nitrosylated in neurodegenerative diseases and *S*-glutathionylated during nitrosative stress (28, 30), but this is the first time, to our knowledge, that the possibility of *S*-glutathionylation of PDI on tyrosine is reported. Our analysis demonstrated that very high concentrations of PN are required to induce UPR; therefore, we think that PDI tyrosine nitrosylation and conjugation of glutathione to oxidized tyrosine are physiologically relevant to plasma membrane and cytosolic pools of PDI. When tyrosine residues within PDI are modified by glutathionylation, it can cause substantial structural changes, mainly an increase in random coil and a decrease in β-sheet, possibly by destroying Tyr aromatic character as can be clearly seen from our structural data (Fig. 5*J*). In other systems, the glutathionylation of Tyr was found to be a reversible reaction, at least in the initial stages of oxidative challenge (86). Therefore, conjugation of glutathione to PN-modified Tyr residues could be a mechanism of oxidative inactivation of the PDI. If not protected by glutathione, oxidized Tyr intermediates can contribute to the formation of intermolecular Cys-Tyr cross-linking and lead to protein aggregation.

It is plausible to assume that irreversible enzymatic activity-damaging modifications are different from the reversible ones. The reversible modifications may participate in redox signaling, which should be activated following CS exposure, as a mechanism of adaptive responses connected to cell toxicity, outcomes of which are dependable on the contest and function of PDI substrates affected by its inactivation (27, 91, 92). This signaling function for PDI during CS exposure is unknown. The irreversible modifications result in the activation of pro-apoptotic UPR, which is heightened with age. In addition, it was suggested that modified PDI acquires a pro-apoptotic function when its levels reach a certain threshold. Here, we demonstrated that the amount of modified PDI increases with the smoker's age. This increase may correlate with an increase in apoptotic cell death seen in COPD smokers.

Further studies are required to clarify whether the PDI modification described here can be detected in lung tissues of chronic smokers and whether their ratio is correlated with the clinical onset of COPD. An increase in the amounts of oxidized PDI correlates with the concomitant increase in apoptotic signaling, accounting, at least partially, for the age-related onset of COPD. This could have a high impact on the field of COPD research and would be a novel approach to understanding COPD.

Author Contributions—A. B. P. and H. K. conceived and designed the study. A. B. P., H. K., Z. W. Y., K. V., K. D. T., and D. M. T. wrote the paper. H. K., K. V., Z. W. Y., X. H. G., D. M. R., and A. B. P. performed and analyzed the experiments.

Acknowledgments—We thank Dr. H. Bose and Dr. M. Prasad for their help with CD experiments. Special thanks to Dr. Maria Hatzoglou for invaluable support, critical reading, and advice on the manuscript as well as for financially supporting the work of X. H. G.

References

1. Vos, T., Flaxman, A. D., Naghavi, M., Lozano, R., Michaud, C., Ezzati, M., Shibuya, K., Salomon, J. A., Abdalla, S., Aboyans, V., Abraham, J., Ackerman, I., Aggarwal, R., Ahn, S. Y., Ali, M. K., et al. (2012) Years lived with disability (YLDs) for 1160 sequelae of 289 diseases and injuries 1990–2010: a systematic analysis for the Global Burden of Disease Study 2010. *Lancet* **380,** 2163–2196
2. Lozano, R., Naghavi, M., Foreman, K., Lim, S., Shibuya, K., Aboyans, V., Abraham, J., Adair, T., Aggarwal, R., Ahn, S. Y., Alvarado, M., Anderson, H. R., Anderson, L. M., Andrews, K. G., Atkinson, C., et al. (2012) Global and regional mortality from 235 causes of death for 20 age groups in 1990 and 2010: a systematic analysis for the Global Burden of Disease Study 2010. *Lancet* **380,** 2095–2128
3. World Health Organization (2013) The 10 leading causes of death in the world, 2000 and 2011. World Health Organization, Geneva, Switzerland
4. Mannino, D. M., and Kiriz, V. A. (2006) Changing the burden of COPD mortality. *Int. J. Chron. Obstruct. Pulmon. Dis.* **1,** 219–233
5. Chung, K. F., and Adcock, I. M. (2008) Multifaceted mechanisms in COPD: inflammation, immunity, and tissue repair and destruction. *Eur. Respir. J.* **31,** 1334–1356
6. Shapiro, S. D., and Ingenito, E. P. (2005) The pathogenesis of chronic obstructive pulmonary disease. *Am. J. Respir. Cell Mol. Biol.* **32,** 367–372
7. Jorgensen, E., Stinson, A., Shan, L., Yang, J., Gietl, D., and Albino, A. P. (2008) Cigarette smoke induces endoplasmic reticulum stress and the unfolded protein response in normal and malignant human lung cells. *BMC Cancer* **8,** 229
8. Hengstermann, A., and Müller, T. (2008) Endoplasmic reticulum stress induced by aqueous extracts of cigarette smoke in 3T3 cells activates the unfolded-protein-response-dependent PERK pathway of cell survival. *Free Radic. Biol. Med.* **44,** 1097–1107
9. Tagawa, Y., Hiramatsu, N., Kasai, A., Hayakawa, K., Okamura, M., Yao, J., and Kitamura, M. (2008) Induction of apoptosis by cigarette smoke via ROS-dependent endoplasmic reticulum stress and CCAAT/enhancer-binding protein-homologous protein (CHOP). *Free Radic. Biol. Med.* **45,** 50–59
10. Kelsen, S. G., Duan, X., Ji, R., Perez, O., Liu, C., and Merali, S. (2008) Cigarette smoke induces an unfolded protein response in the human lung: a proteomic approach. *Am. J. Respir. Cell Mol. Biol.* **38,** 541–550
11. Geraghty, P., Wallace, A., and D'Armiento, J. M. (2011) Induction of the unfolded protein response by cigarette smoke is primarily an activating transcription factor 4-C/EBP homologous protein mediated process. *Int. J. Chron. Obstruct. Pulmon. Dis.* **6,** 309–319
12. Huang, C., Wang, J. J., Ma, J. H., Jin, C., Yu, Q., and Zhang, S. X. (2015) Activation of the UPR protects against cigarette smoke-induced RPE apoptosis through up-regulation of Nrf2. *J. Biol. Chem.* **290,** 5367–5380
13. Gan, G., Hu, R., Dai, A., Tan, S., Ouyang, Q., Fu, D., and Jiang, D. (2011) The role of endoplasmic reticulum stress in emphysema results from cigarette smoke exposure. *Cell. Physiol. Biochem.* **28,** 725–732
14. Malhotra, D., Thimmulappa, R., Vij, N., Navas-Acien, A., Sussan, T., Merali, S., Zhang, L., Kelsen, S. G., Myers, A., Wise, R., Tuder, R., and Biswal, S. (2009) Heightened endoplasmic reticulum stress in the lungs of patients with chronic obstructive pulmonary disease: the role of Nrf2-regulated proteasomal activity. *Am. J. Respir. Crit. Care Med.* **180,** 1196–1207
15. Schröder, M., and Kaufman, R. J. (2005) ER stress and the unfolded protein response. *Mutat. Res.* **569,** 29–63
16. Shore, G. C., Papa, F. R., and Oakes, S. A. (2011) Signaling cell death from the endoplasmic reticulum stress response. *Curr. Opin. Cell Biol.* **23,** 143–149
17. Wu, J., and Kaufman, R. (2006) From acute ER stress to physiological roles of the Unfolded Protein Response. *Cell Death Differ.* **13,** 374–384

18. Kenche, H., Baty, C. J., Vedagiri, K., Shapiro, S. D., and Blumental-Perry, A. (2013) Cigarette smoking affects oxidative protein folding in endoplasmic reticulum by modifying protein-disulfide isomerase. *FASEB J.* **27,** 965–977
19. Townsend, D. M., Manevich, Y., He, L., Xiong, Y., Bowers, R. R., Jr., Hutchens, S., and Tew, K. D. (2009) Nitrosative stress-induced *S*-glutathionylation of protein-disulfide isomerase leads to activation of the unfolded protein response. *Cancer Res.* **69,** 7626–7634
20. Grek, C., and Townsend, D. M. (2014) Protein-disulfide isomerase superfamily in disease and the regulation of apoptosis. *Endoplasmic Reticulum Stress Dis.* **1,** 4–17
21. Jessop, C. E., Chakravarthi, S., Watkins, R. H., and Bulleid, N. J. (2004) Oxidative protein folding in the mammalian endoplasmic reticulum. *Biochem. Soc. Trans.* **32,** 655–658
22. Turano, C., Coppari, S., Altieri, F., and Ferraro, A. (2002) Proteins of the PDI family: unpredicted non-ER locations and functions. *J. Cell. Physiol.* **193,** 154–163
23. Tian, G., Kober, F. X., Lewandrowski, U., Sickmann, A., Lennarz, W. J., and Schindelin, H. (2008) The catalytic activity of protein-disulfide isomerase requires a conformationally flexible molecule. *J. Biol. Chem.* **283,** 33630–33640
24. Benham, A. M. (2012) The protein-disulfide isomerase family: key players in health and disease. *Antioxid. Redox Signal.* **16,** 781–789
25. Lumb, R. A., and Bulleid, N. J. (2002) Is protein-disulfide isomerase a redox-dependent molecular chaperone? *EMBO J.* **21,** 6763–6770
26. Jacob, C., Battaglia, E., Burkholz, T., Peng, D., Bagrel, D., and Montenarh, M. (2012) Control of oxidative post-translational cysteine modifications: from intricate chemistry to widespread biological and medical applications. *Chem. Res. Toxicol.* **25,** 588–604
27. Nakamura, T., and Lipton, S. A. (2013) Emerging role of protein-protein transnitrosylation in cell signaling pathways. *Antioxid. Redox Signal.* **18,** 239–249
28. Uehara, T., Nakamura, T., Yao, D., Shi, Z. Q., Gu, Z., Ma, Y., Masliah, E., Nomura, Y., and Lipton, S. A. (2006) *S*-Nitrosylated protein-disulphide isomerase links protein misfolding to neurodegeneration. *Nature* **441,** 513–517
29. Muller, C., Bandemer, J., Vindis, C., Camaré, C., Mucher, E., Guéraud, F., Larroque-Cardoso, P., Bernis, C., Auge, N., Salvayre, R., and Negre-Salvayre, A. (2013) Protein-disulfide isomerase modification and inhibition contribute to ER stress and apoptosis induced by oxidized low density lipoproteins. *Antioxid. Redox Signal.* **18,** 731–742
30. Townsend, D. M. (2007) *S*-Glutathionylation: indicator of cell stress and regulator of the unfolded protein response. *Mol. Interv.* **7,** 313–324
31. Gutiérrez, T., and Simmen, T. (2014) Endoplasmic reticulum chaperones and oxidoreductases: critical regulators of tumor cell survival and immunorecognition. *Front. Oncol.* **4,** 291
32. Parakh, S., and Atkin, J. D. (2015) Novel roles for protein disulphide isomerase in disease states: a double edged sword? *Front Cell Dev. Biol.* 2015 May 21;3:30
33. Talhout, R., Schulz, T., Florek, E., van Benthem, J., Wester, P., and Opperhuizen, A. (2011) Hazardous compounds in tobacco smoke. *Int. J. Environ. Res. Public Health* **8,** 613–628
34. Church, D. F., and Pryor, W. A. (1985) Free-radical chemistry of cigarette smoke and its toxicological implications. *Environ. Health Perspect.* **64,** 111–126
35. Muller, T., Haussmann, H. J., and Schepers, G. (1997) Evidence for peroxynitrite as an oxidative stress-inducing compound of aqueous cigarette smoke fractions. *Carcinogenesis* **18,** 295–301
36. Chouchane, S., Wooten, J. B., Tewes, F. J., Wittig, A., Müller, B. P., Veltel, D., and Diekmann, J. (2006) Involvement of semiquinone radicals in the *in vitro* cytotoxicity of cigarette mainstream smoke. *Chem. Res. Toxicol.* **19,** 1602–1610
37. Faux, S. P., Tai, T., Thorne, D., Xu, Y., Breheny, D., and Gaca, M. (2009) The role of oxidative stress in the biological responses of lung epithelial cells to cigarette smoke. *Biomarkers* **14,** 90–96
38. Margittai, É., Enyedi, B., Csala, M., Geiszt, M., and Bánhegyi, G. (2015) Composition of the redox environment of the endoplasmic reticulum and sources of hydrogen peroxide. *Free Radic. Biol. Med.* **83,** 331–340
39. Margittai, É., Löw, P., Stiller, I., Greco, A., Garcia-Manteiga, J. M., Pengo, N., Benedetti, A., Sitia, R., and Bánhegyi, G. (2012) Production of H(2)O(2) in the endoplasmic reticulum promotes *in vivo* disulfide bond formation. *Antioxid. Redox Signal.* **16,** 1088–1099
40. Sato, Y., Kojima, R., Okumura, M., Hagiwara, M., Masui, S., Maegawa, K., Saiki, M., Horibe, T., Suzuki, M., and Inaba, K. (2013) Synergistic cooperation of PDI family members in peroxiredoxin 4-driven oxidative protein folding. *Sci. Rep.* **3,** 2456
41. Kabiraj, P., Marin, J. E., Varela-Ramirez, A., Zubia, E., and Narayan, M. (2014) Ellagic acid mitigates SNO-PDI induced aggregation of Parkinsonian biomarkers. *ACS Chem. Neurosci.* **5,** 1209–1220
42. Carp, H., and Janoff, A. (1978) Possible mechanisms of emphysema in smokers. *In vitro* suppression of serum elastase-inhibitory capacity by fresh cigarette smoke and its prevention by antioxidants. *Am. Rev. Respir. Dis.* **118,** 617–621
43. Borenfreund, E., and Puerner, J. A. (1985) Toxicity determined *in vitro* by morphological alterations and neutral red absorption. *Toxicol. Lett.* **24,** 119–124
44. Molteni, S. N., Fassio, A., Ciriolo, M. R., Filomeni, G., Pasqualetto, E., Fagioli, C., and Sitia, R. (2004) Glutathione limits Ero1-dependent oxidation in the endoplasmic reticulum. *J. Biol. Chem.* **279,** 32667–32673
45. Watanabe, M. M., Laurindo, F. R., and Fernandes, D. C. (2014) Methods of measuring protein-disulfide isomerase activity: a critical overview. *Front. Chem.* **2,** 73
46. Heuck, A. P., and Wolosiuk, R. A. (1997) Di-fluoresceinthiocarbamyl-insulin: a fluorescent substrate for the assay of protein disulfide oxidoreductase activity. *Anal. Biochem.* **248,** 94–101
47. Maeda, R., Ado, K., Takeda, N., and Taniguchi, Y. (2007) Promotion of insulin aggregation by protein disulfide isomerase. *Biochim. Biophys. Acta.* **1774,** 1619–1627
48. Ben Khalaf, N., De Muylder, G., Ratnam, J., Kean-Hooi Ang, K., Arkin, M., McKerrow, J., and Chenik, M. (2011) A high-throughput turbidometric assay for screening inhibitors of *Leishmania major* protein-disulfide isomerase. *J. Biomol. Screen.* **16,** 545–551
49. Smith, A. M., Chan, J., Oksenberg, D., Urfer, R., Wexler, D. S., Ow, A., Gao, L., McAlorum, A., and Huang, S. G. (2004) A high-throughput turbidometric assay for screening inhibitors of protein-disulfide isomerase activity. *J. Biomol. Screen.* **9,** 614–620
50. Walker, K. W., Lyles, M. M., and Gilbert, H. F. (1996) Catalysis of oxidative protein folding by mutants of protein-disulfide isomerase with a single active-site cysteine. *Biochemistry* **35,** 1972–1980
51. Wani, R., Qian, J., Yin, L., Bechtold, E., King, S. B., Poole, L. B., Paek, E., Tsang, A. W., and Furdui, C. M. (2011) Isoform-specific regulation of Akt by PDGF-induced reactive oxygen species. *Proc. Natl. Acad. Sci. U.S.A.* **108,** 10550–10555
52. Moretto, N., Bertolini, S., Iadicicco, C., Marchini, G., Kaur, M., Volpi, G., Patacchini, R., Singh, D., and Facchinetti, F. (2012) Cigarette smoke and its component acrolein augment IL-8/CXCL8 mRNA stability via p38 MAPK/MK2 signaling in human pulmonary cells. *Am. J. Physiol. Lung Cell. Mol. Physiol.* **303,** L929–L938
53. Sharma, A., Patil, J. A., Gramajo, A. L., Seigel, G. M., Kuppermann, B. D., and Kenney, C. M. (2012) Effects of hydroquinone on retinal and vascular cells *in vitro*. *Indian J. Ophthalmol.* **60,** 189–193
54. Chen, Q., and Ames, B. N. (1994) Senescence-like growth arrest induced by hydrogen peroxide in human diploid fibroblast F65 cells. *Proc. Natl. Acad. Sci. U.S.A.* **91,** 4130–4134
55. Hautamaki, R. D., Kobayashi, D. K., Senior, R. M., and Shapiro, S. D. (1997) Requirement for macrophage elastase for cigarette smoke-induced emphysema in mice. *Science* **277,** 2002–2004
56. Rehder, D. S., and Borges, C. R. (2010) Cysteine sulfenic acid as an intermediate in disulfide bond formation and nonenzymatic protein folding. *Biochemistry* **49,** 7748–7755
57. Rehder, D. S., and Borges, C. R. (2010) Possibilities and pitfalls in quantifying the extent of cysteine sulfenic acid modification of specific proteins within complex biofluids. *BMC Biochem.* **11,** 25
58. Fasman, G. D. (1996) in *Circular Dichroism and The Conformational Analysis of Biomolecules* (Fasman, G. D., ed) pp. 1–738, Plenum Press, New York

59. Sreerama, N., and Woody, R. W. (2004) Computation and analysis of protein circular dichroism spectra. *Methods Enzymol.* **383,** 318–351
60. Anelli, T., and Sitia, R. (2008) Protein quality control in the early secretory pathway. *EMBO J.* **27,** 315–327
61. Zhao, G., Lu, H., and Li, C. (2015) Proapoptotic activities of protein-disulfide isomerase (PDI) and PDIA3 protein, a role of the Bcl-2 protein Bak. *J. Biol. Chem.* **290,** 8949–8963
62. Mercado, N., Ito, K., and Barnes, P. J. (2015) Accelerated ageing of the lung in COPD: new concepts. *Thorax* **70,** 482–489
63. Morissette, M. C., Parent, J., and Milot, J. (2009) Alveolar epithelial and endothelial cell apoptosis in emphysema: what we know and what we need to know. *Int. J. Chron. Obstruct. Pulmon. Dis.* **4,** 19–31
64. Henson, P. M., Vandivier, R. W., and Douglas, I. S. (2006) Cell death, remodeling, and repair in chronic obstructive pulmonary disease? *Proc. Am. Thorac. Soc.* **3,** 713–717
65. Xu, S., Sankar, S., and Neamati, N. (2014) Protein-disulfide isomerase: a promising target for cancer therapy. *Drug Discov. Today* **19,** 222–240
66. Greenbaum, D., Colangelo, C., Williams, K., and Gerstein, M. (2003) Comparing protein abundance and mRNA expression levels on a genomic scale. *Genome Biol.* **4,** 117
67. Khositseth, S., Pisitkun, T., Slentz, D. H., Wang, G., Hoffert, J. D., Knepper, M. A., and Yu, M. J. (2011) Quantitative protein and mRNA profiling shows selective post-transcriptional control of protein expression by vasopressin in kidney cells. *Mol. Cell. Proteomics* **10,** M110.004036
68. Washburn, M. P., Koller, A., Oshiro, G., Ulaszek, R. R., Plouffe, D., Deciu, C., Winzeler, E., and Yates, J. R., 3rd. (2003) Protein pathway and complex clustering of correlated mRNA and protein expression analyses in *Saccharomyces cerevisiae*. *Proc. Natl. Acad. Sci. U.S.A.* **100,** 3107–3112
69. Labunskyy, V. M., Gerashchenko, M. V., Delaney, J. R., Kaya, A., Kennedy, B. K., Kaeberlein, M., and Gladyshev, V. N. (2014) Lifespan extension conferred by endoplasmic reticulum secretory pathway deficiency requires induction of the unfolded protein response. *PLoS Genet.* **10,** e1004019
70. Krishnan, K., Ren, Z., Losada, L., Nierman, W. C., Lu, L. J., and Askew, D. S. (2014) Polysome profiling reveals broad translatome remodeling during endoplasmic reticulum (ER) stress in the pathogenic fungus *Aspergillus fumigatus*. *BMC Genomics* **15,** 159
71. Ohba, H., Harano, T., and Omura, T. (1981) Biosynthesis and turnover of a microsomal protein-disulfide isomerase in rat liver. *J. Biochem.* **89,** 901–907
72. Meiners, S., and Eickelberg, O. (2012) What shall we do with the damaged proteins in lung disease? Ask the proteasome! *Eur. Respir. J.* **40,** 1260–1268
73. Meiners, S., vanRijt, S., Hauck, S., Dahimann, B., and Eickelberg, O. (2011) American Thoracic Society International Conference, Denver, CO, May 13–18, 2011, American Thoracic Society, New York
74. Yang, H., Yang, S., Liu, J., Shao, F., Wang, H., and Wang, Y. (2015) The association of GSTM1 deletion polymorphism with lung cancer risk in Chinese population: evidence from an updated meta-analysis. *Sci. Rep.* **5,** 9392
75. Mota, P., Silva, H. C., Soares, M. J., Pego, A., Loureiro, M., Cordeiro, C. R., and Regateiro, F. J. (2015) Genetic polymorphisms of phase I and phase II metabolic enzymes as modulators of lung cancer susceptibility. *J. Cancer Res. Clin. Oncol.* **141,** 851–860
76. Chen, H. C., Cao, Y. F., Hu, W. X., Liu, X. F., Liu, Q. X., Zhang, J., and Liu, J. (2006) Genetic polymorphisms of phase II metabolic enzymes and lung cancer susceptibility in a population of Central South China. *Dis. Markers* **22,** 141–152
77. Lakhdar, R., Denden, S., Kassab, A., Leban, N., Knani, J., Lefranc, G., Miled, A., Chibani, J. B., and Khelil, A. H. (2011) Update in chronic obstructive pulmonary disease: role of antioxidant and metabolizing gene polymorphisms. *Exp. Lung Res.* **37,** 364–375
78. Yan, F., Chen, C., Jing, J., Li, W., Shen, H., and Wang, X. (2010) Association between polymorphism of glutathione *S*-transferase P1 and chronic obstructive pulmonary disease: a meta-analysis. *Respir. Med.* **104,** 473–480
79. Lu, B., and He, Q. (2002) Correlation between exon5 polymorphism of glutathione S-transferase P1 gene and susceptibility to chronic obstructive pulmonary disease in northern Chinese population of Han nationality living in Beijing, China. *Zhonghua Nei Ke Za Zhi* **41,** 678–681
80. Ishii, T., Matsuse, T., Teramoto, S., Matsui, H., Miyao, M., Hosoi, T., Takahashi, H., Fukuchi, Y., and Ouchi, Y. (1999) Glutathione *S*-transferase P1 (GSTP1) polymorphism in patients with chronic obstructive pulmonary disease. *Thorax* **54,** 693–696
81. Roth, D. M., and Balch, W. E. (2011) Modeling general proteostasis: proteome balance in health and disease. *Curr. Opin. Cell Biol.* **23,** 126–134
82. Balch, W. E., Morimoto, R. I., Dillin, A., and Kelly, J. W. (2008) Adapting proteostasis for disease intervention. *Science* **319,** 916–919
83. Bodas, M., Min, T., and Vij, N. (2011) Critical role of CFTR-dependent lipid rafts in cigarette smoke-induced lung epithelial injury. *Am. J. Physiol. Lung Cell. Mol. Physiol.* **300,** L811–L820
84. Dahl, J. U., Gray, M. J., and Jakob, U. (2015) Protein quality control under oxidative stress conditions. *J. Mol. Biol.* **427,** 1549–1563
85. Morimoto, R. I., and Cuervo, A. M. (2014) Proteostasis and the aging proteome in health and disease. *J. Gerontol. A. Biol. Sci. Med. Sci.* **69,** S33–S38
86. Lin, D., Saleh, S., and Liebler, D. C. (2008) Reversibility of covalent electrophile-protein adducts and chemical toxicity. *Chem. Res. Toxicol.* **21,** 2361–2369
87. Hodge, S., Matthews, G., Mukaro, V., Ahern, J., Shivam, A., Hodge, G., Holmes, M., Jersmann, H., and Reynolds, P. N. (2011) Cigarette smoke-induced changes to alveolar macrophage phenotype and function are improved by treatment with procysteine. *Am. J. Respir. Cell Mol. Biol.* **44,** 673–681
88. Hakim, I. A., Harris, R. B., Chow, H. H., Dean, M., Brown, S., and Ali, I. U. (2004) Effect of a 4-month tea intervention on oxidative DNA damage among heavy smokers: role of glutathione *S*-transferase genotypes. *Cancer Epidemiol. Biomarkers Prev.* **13,** 242–249
89. Pendyala, L., Schwartz, G., Bolanowska-Higdon, W., Hitt, S., Zdanowicz, J., Murphy, M., Lawrence, D., and Creaven, P. J. (2001) Phase I/pharmacodynamic study of *N*-acetylcysteine/oltipraz in smokers: early termination due to excessive toxicity. *Cancer Epidemiol. Biomarkers Prev.* **10,** 269–272
90. Nagy, P., Lechte, T. P., Das, A. B., and Winterbourn, C. C. (2012) Conjugation of glutathione to oxidized tyrosine residues in peptides and proteins. *J. Biol. Chem.* **287,** 26068–26076
91. Haendeler, J. (2006) Thioredoxin-1 and post-translational modifications. *Antioxid. Redox Signal.* **8,** 1723–1728
92. Shao, D., Oka, S., Brady, C. D., Haendeler, J., Eaton, P., and Sadoshima, J. (2012) Redox modification of cell signaling in the cardiovascular system. *J. Mol. Cell. Cardiol.* **52,** 550–558
93. Da Violante, G., Zerrouk, N., Richard, I., Provot, G., Chaumeil, J. C., and Arnaud, P. (2002) Evaluation of the cytotoxicity effect of dimethyl sulfoxide (DMSO) on Caco2/TC7 colon tumor cell cultures. *Biol. Pharm. Bull.* **25,** 1600–1603
94. Qi, W., Ding, D., and Salvi, R. J. (2008) Cytotoxic effects of dimethyl sulphoxide (DMSO) on cochlear organotypic cultures. *Hear. Res.* **236,** 52–60